PIPE DREAMS: EVALUATION OF OCEAN CO_2 INJECTION AS A MEANS FOR REDUCING ATMOSPHERIC CARBON DIOXIDE CONCENTRATIONS

by

Thomas J. Rodengen
B.A., University of St. Thomas 2007
B.S., University of St. Thomas 2007

RESEARCH PROJECT SUBMITTED IN
PARTIAL FULFILMENT OF
THE REQUIREMENTS FOR THE DEGREE OF

MASTER OF RESOURCE MANAGEMENT

In the
School of Resource and Environmental Management

Report No. 486

SIMON FRASER UNIVERSITY

Fall 2009

APPROVAL

Name:	Thomas Rodengen
Degree:	Master of Resource Management
Title of Research Project:	Pipe Dreams: Evaluation of Ocean CO_2 Injection as a Means for Reducing Atmospheric Carbon Dioxide Concentrations
Project No.:	486
Examining Committee:	
Chair:	Bradford Griffin Resource Management Candidate
	_____
	Dr. Karen Kohfeld Senior Supervisor Assistant Professor, School of Resource and Environmental Management, Simon Fraser University
	_____
	Dr. Andy Ridgwell Supervisor Leader of BRIDGE, Royal Society University Research Fellow, School of Geographical Sciences, University of Bristol
	_____
	Dr. Murray Rutherford Supervisor Associate Professor, School of Resource and Environmental Management, Simon Fraser University
Date Defended/Approved:	_____

Abstract

Deep ocean injection of carbon dioxide (CO_2) has been proposed as one means of dealing with the build-up of anthropogenic CO_2 in the atmosphere. This study used a series of Earth System Model experiments to inject an idealized pulse of CO_2 into each ocean grid cell to assess the efficiency of each location in storing CO_2 over a 1,000 year period relative to how that CO_2 would enter the ocean naturally. Potential injection sites were selected based on a series of criteria, including physical constraints, technological capability for access, and socio-environmental importance to society. After these restrictions were applied, 19 sites were identified, possessing relative efficiencies between 60 to 100% by year 200 and -7 to 9% by year 1,000. Carbon sequestration costs for the 19 eligible injection sites range from US$75.55 to US$1054.75/ton CO_2 net stored, which is not competitive with other carbon sequestration options at this time.

Keywords: CO_2; climate change; CCS; ocean storage; ocean sequestration; ocean injection

Dedication

For my parents

Acknowledgements

Particular thanks goes to Dr. Karen Kohfeld, my graduate supervisor who provided guidance and support every single step of the way.

Dr. Andy Ridgwell also deserves recognition for his advising and guidance through the wonderful world of the GENIE model.

Special thanks goes to Dr. Murray Rutherford for his valuable feedback and insight regarding decision analysis as well as his editing suggestions and to Dr. John Nyboer who provided direction on economic matters

Thanks to the support of my colleagues Brad Griffin for aid in data analysis and Stu Johnson for editing and general support. Finally, thank you to the enduring love and support of my partner, Nina Mostegl.

Table of Contents

List of Figures

List of Tables

1. INTRODUCTION

Climate models indicate that carbon dioxide (CO_2) emissions from the burning of fossil fuels have a significant effect on climate change [*IPCC,* 2007]. Dealing with the effects of anthropogenic climate change remains a major political, economic, and technological challenge. In recent years, the field of geo-engineering has brought forth a wide range of technological solutions designed to deal with climate change, ranging from bio-engineered high-albedo plant leaves [*Ridgwell et al.,* 2009] to sulfate injection into the stratosphere [*Kravitz et al.,* 2009]. While these options are intended to address the damaging effects of climate change, they would have little impact on other problems associated with excessive CO_2 emissions. For example, high-CO_2 concentrations are expected to acidify the ocean [*Doney et al.,* 2009], creating substantial damage to calcifying organisms (e.g. corals) and associated marine ecosystems [*Guinotte and Fabry,* 2008]. Several mitigation options have been proposed to curb fossil fuel emissions of CO_2, including a range of policy and technological approaches [*IPCC,* 2007].
Most integrated assessment models show a demand for 2,220 Gigatons (Gt) CO_2 of storage over the course of this century to stabilize atmospheric CO_2 between 450-750 parts per million (ppm) [*Dooley,* 2006] (Figure 1). Stabilization between 450-750 ppm corresponds roughly to a doubling of CO_2 in the atmosphere relative to preindustrial levels and represents the most common set of targets discussed in previous literature [*Clarke et al.,* 2009].

Carbon Capture and Storage (CCS) is one possible technological method that has received special attention from the Intergovernmental Panel on Climate Change [*IPCC,* 2005], as both land and ocean reservoirs have the potential to store carbon that is captured from point sources such as power plants. Most attention has focused on the potential of geologic storage where CO_2 can be stored in depleted or depleting oil and gas fields, deep saline aquifers, and unmineable coal seams. Estimates currently place the geologic storage capacity at 11,000 Gt CO_2, approximately 10,000 Gt CO_2 of which would come from deep saline aquifers [*Dooley et al.,* 2006] (Figure 2). To date, three large-scale geologic storage efforts have demonstrated the possible viability of future geologic storage projects. The In Salah Project in Algeria and the Weyburn Project in

Canada are terrestrial oil and gas reservoirs where approximately 17 Megatons (Mt) CO_2 and 20 Mt CO_2 are planned to be stored over the lifetime of the projects, respectively. The Sleipner project in Norway is an offshore oil and gas reservoir where an estimated 20 Mt CO2 are expected to be stored [*ISEE,* 2008].

Geologic storage has both advantages and disadvantages. While the total, potential capacity of geologic storage is seemingly greater than the total demand based on stabilization targets, geologic storage has the obstacle of a scattered distribution of storage sites with varied efficiencies. Another possible advantage is that pumping CO_2 into existing oil fields can actually enhance oil recovery. However, the stored CO_2 may leak from improperly plugged wellbores or corroded reservoir walls. Additionally, seismic activity may create CO_2 leakages resulting in the acidification of groundwater resources. If discharged on land, CO_2 presents an asphyxiation hazard [*Pruess,* 2007]. Finally, concerns over the public's acceptance and the current lack of proper policies and regulatory frameworks will be major barriers to large-scale deployment of storage [*Bachu,* 2007].

Figure 1. Stabilization pathways of greenhouse gas emissions for meeting various atmospheric CO_2 concentration targets over the next three centuries [taken from *Edmonds*, 2008]

X axis measured in years. Stabilization emissions targets are measured in Gigatons carbon (Gt C) and are derived to meet a given atmospheric CO_2 ppm level. For example, "GTSP_550" is atmospheric CO_2 stabilization at 550 ppm, which allows global annual carbon emissions to peak at ~10.5 Gt in year 2050. Also depicted are historical emissions (black line) and a reference (red line), business-as-usual, case.

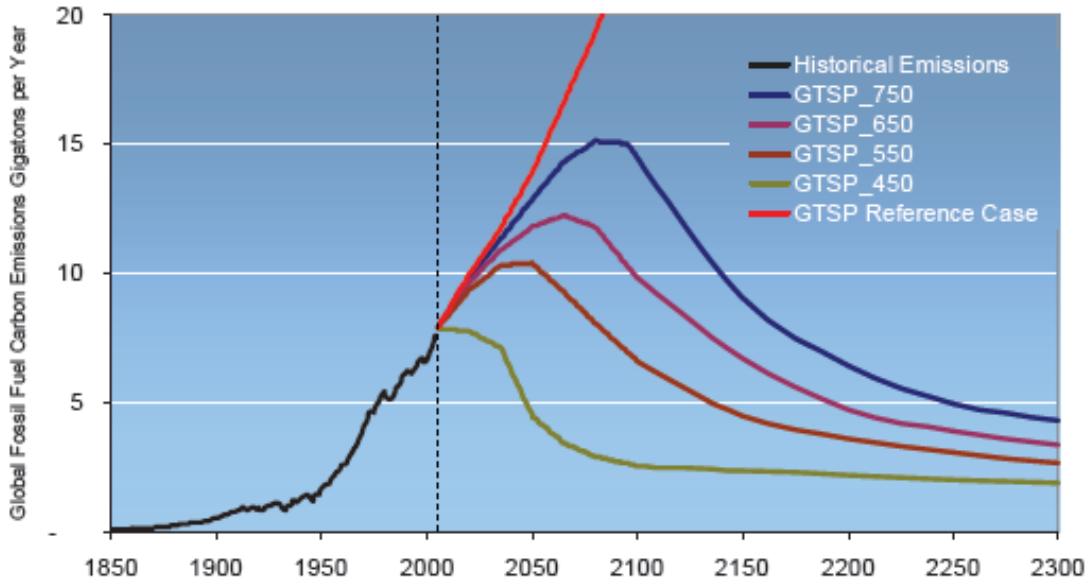

Figure 2. Aggregate potential capacity for various geological storage technologies [redrawn from *Edmonds*, 2008]

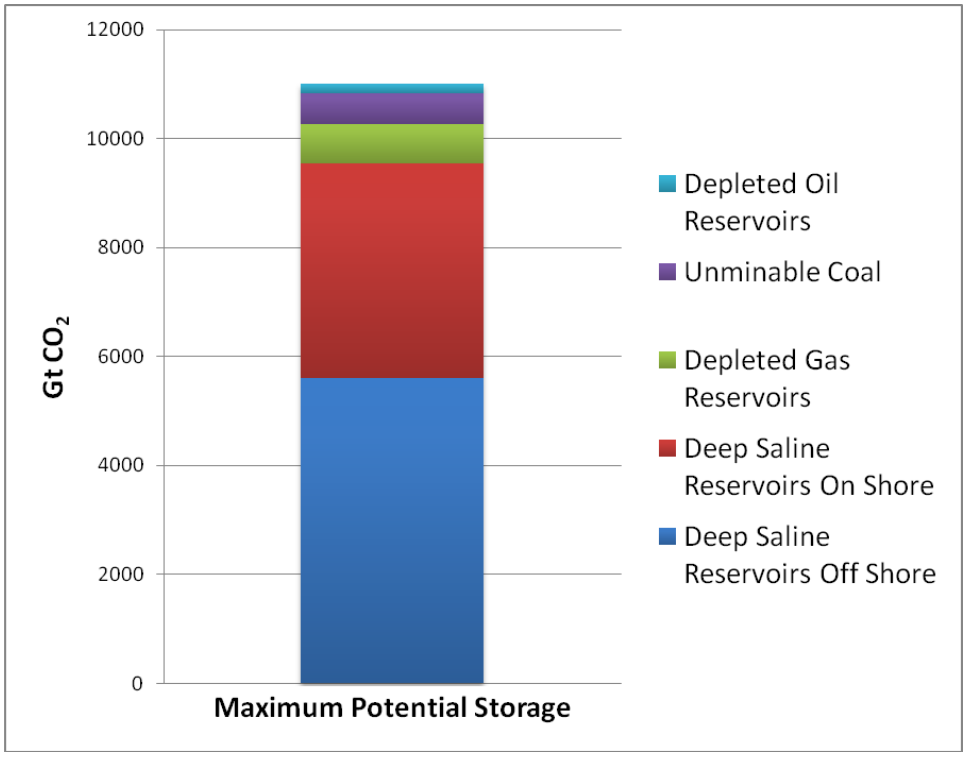

Another sequestration option for CO_2 is storage in the ocean, which involves capturing CO_2, compressing it into liquid form, and subsequently transporting and injecting it into the ocean. Marchetti [1977] first proposed that liquefied CO_2 would sink to the seafloor if the injection depth were deep enough to make the injected CO_2 denser than the surrounding seawater. At average ocean temperature and pressure, CO_2 is in a gaseous phase above 400-500 m and a liquid phase below approximately 400-500 m (Figure 3). Liquid CO_2 is more easily compressed than seawater, and at a depth of 3,000 m, its density becomes the same as that of seawater. Below 3,000 m, liquefied CO_2 will sink, and therefore have the potential to be stored out of contact from the atmosphere (Figure 4). The effectiveness of this, and any other, storage method at sequestering CO_2 is gauged by how long this CO_2 remains isolated from the atmosphere [*Herzog et al.*, 2003].

Figure 3. CO_2 sea water phase diagram [redrawn from *Brewer et al.*, 2004]

CO_2 is stable in the liquid phase below the blue line and stable in a gas phase above the blue line. The black line represents average global ocean temperature changes with depth [*NOAA*, 2008]. Below the red line, CO_2 reacts with seawater to form a solid, ice-like hydrate (CO_2*$6H_2O$).

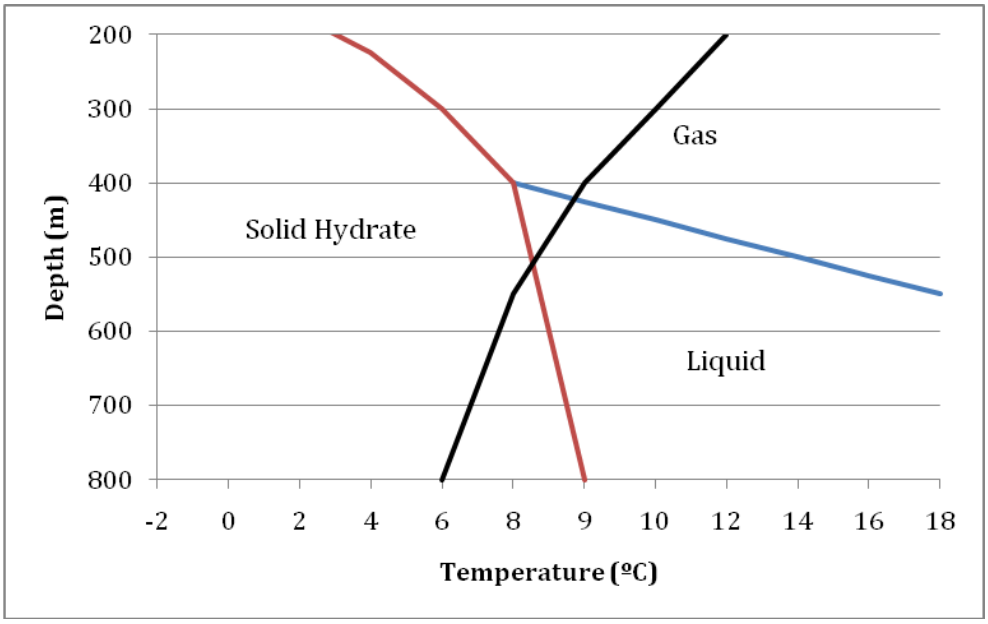

Figure 4. Graph of depth versus seawater density (g/cm^3) demonstrating the typical behavior of liquid CO_2 between ocean depths of 2,000 and 3,500 m depth[redrawn from *IPCC*, 2005]

Black line represents average ocean density [*NOAA*, 2008]. Deeper than 3,000 m, liquid CO_2 is denser than sea water, and thus sinks to the bottom. Shallower than 2,500 m, liquid CO_2 is less dense than sea water, and thus floats to the surface. Between these two depths, the fate of liquid CO_2 varies with location.

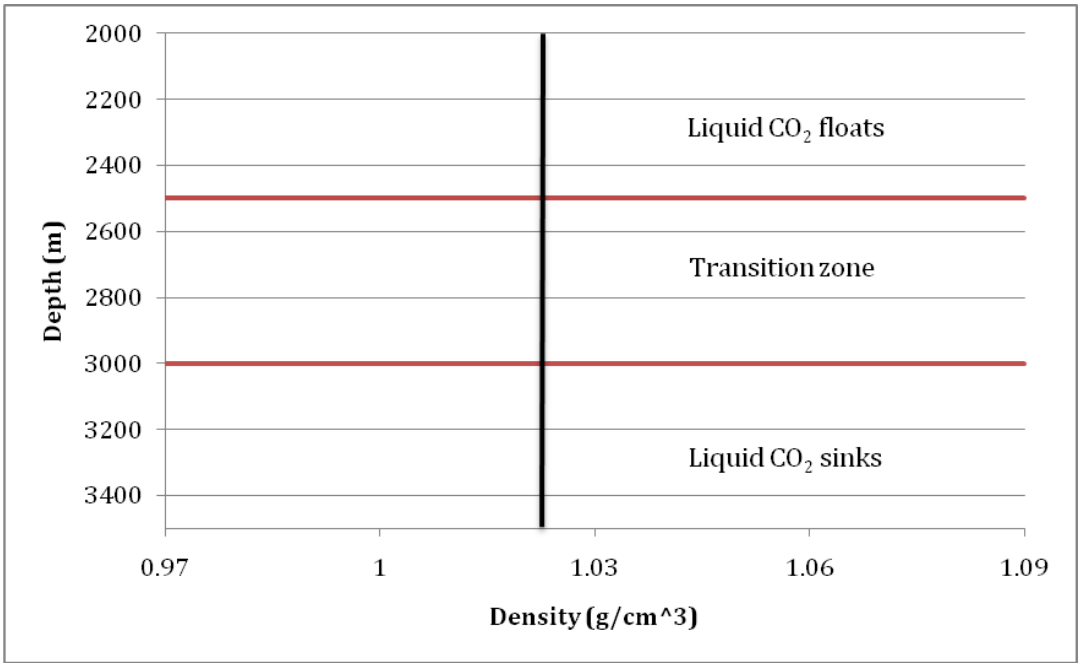

Ocean models have been used to predict the effectiveness of liquefied CO_2 storage in the ocean by simulating the fate of CO_2 following its injection. Eight modeling groups performed a variety of 3-dimensional ocean model simulations in which 367 Mt/y of CO_2 were injected over the course of 100 years at seven different sites (Bay of Biscay, New York, Rio de Janeiro, San Francisco, Tokyo, Jakarta and Mumbai), at three different water depths (899 m, 1,500 m and 3,000 m) for 500 years [*Orr*, 2004]. These models revealed that the deeper injections (1,500 m and 3,000 m) of CO_2 were isolated from the atmosphere for longer durations (>100 years). While not all the models agreed, the Pacific sites (San Francisco and Tokyo) generally retained 35% of the initially injected CO_2, which is 10% greater than sites in the Atlantic and Indian Oceans over the 500-year model run. Furthermore, sites close to the Southern Ocean (Rio de Janeiro and Jakarta) retained less CO_2 (20%) during the 500-year time period. Caldeira and Wickett (2005) investigated the impact of ocean injection on ocean chemistry at these same sites. They

concluded that deep ocean injection was likely to create substantial changes in the surrounding deep water chemistry as 'the price' for reducing the effects of CO_2 on surface ocean acidification and anthropogenic climate change [*Caldeira and Wickett*, 2005].

These modeling studies have provided a first-order notion of the potential effectiveness and environmental costs of ocean CO_2 injection at several locations. However, these studies did not provide an objective analysis of every location in the ocean in order to find the most effective locations for ocean carbon storage. These studies also did not place the potential for ocean injection in the context of environmental, social, or economic issues. In the present study, an ensemble of Earth system model (GENIE-1) simulations is used to examine CO_2 storage efficiency at every location in the ocean over the course of 1,000 years. In order to address the practicality of planned ocean CO_2 injection, a subset of the sites that are most likely to be suitable for sequestration is selected based on physical constraints, technological capability to reach these ocean sites, as well as environmental and social criteria. Finally, estimated economic costs for transportation and sequestration at each of the more suitable sites, calculated on the basis of the distance of the site from major CO_2-emitting regions, are presented. In summary, this study provides a whole ocean analysis of potential injection sites. This study is different from previous studies by merit of scale and its multi-disciplinary approach to site selection.

2. METHODS

An ensemble of simulated liquefied CO_2 injection experiments for each site in the ocean was performed using the Grid ENabled Integrated Earth system model (GENIE-1). Injection sites were then screened using a set of physical, technological, and socio-environmental criteria which were added to identify the most feasible potential injection sites. The practical potential of each remaining site for CO_2 sequestration was then evaluated based on (a) its relative efficiency at retaining CO_2 in isolation from the atmosphere (as determined from model simulations), and (b) the estimated potential economic cost (based on its distance from major emitting regions).

2.1 Earth System Model Simulations

The GENIE-1 model is an Earth System model of intermediate complexity designed to address the long-term response of the Earth system to natural and human-induced perturbations. The model is based on the fast climate model of Edwards and Marsh (2005), which features a reduced physics (frictional geostrophic) 3-dimensional ocean circulation model, coupled to a 2-dimensional energy-moisture balance model of the atmosphere and a dynamic thermodynamic sea ice model. This ocean model includes a 2-dimensional atmospheric chemistry module called ATCHEM and a representation of marine carbon cycling called BIOGEM, which is based on a phosphate control of biological productivity and is calibrated against observational data sets of ocean geochemistry [*Ridgwell et al.,* 2007] (Figure 5).

Figure 5. Schematic illustration of GENIE-1 model components and interaction [taken from *Ridgwell and Hargreaves*, 2007]

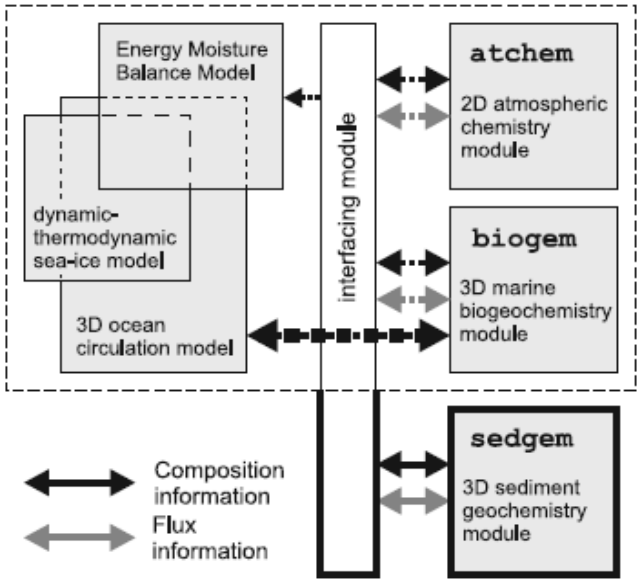

GENIE-1 is an appropriate modeling tool for this study for several reasons. First, its computational efficiency allows thousands of 1,000-year experiments to be conducted in a relative short period of time. Second, GENIE-1 is known to reproduce ocean circulation [*Edwards and Marsh*, 2005], biogeochemical processes [*Ridgwell et al.*, 2007] and ocean tracers [e.g., *Cao et al.*, 2009] with relative accuracy. A model intercomparison study [*Cao et al.*, 2009] showed GENIE-1 to be one of the models that most closely approximates observed rates of ocean uptake of CO_2 (although, like other models, it overestimates oceanic uptake). GENIE-1 does not replicate observed values of anthropogenic CO_2 uptake by the ocean well at the high latitudes (poleward of 62.7º) [*Ridgwell et al.*, 2007].

The model is forced with annual average wind stress and seasonal insolation, and implemented on a 36x36 latitude-longitude grid (10 degree increments in longitude but uniform in sine of latitude, giving ~3.2 degrees latitudinal increments at the equator increasing to 19.2 degrees in the highest latitude band). The ocean has 16 vertical (z-coordinate) levels (Figure 6), and various tracers. These tracers are advected, diffused and convected on-line by the ocean circulation.

Figure 6. Ocean bathymetry of the GENIE-1 model [taken from *Ridgwell and Hargreaves*, 2007]

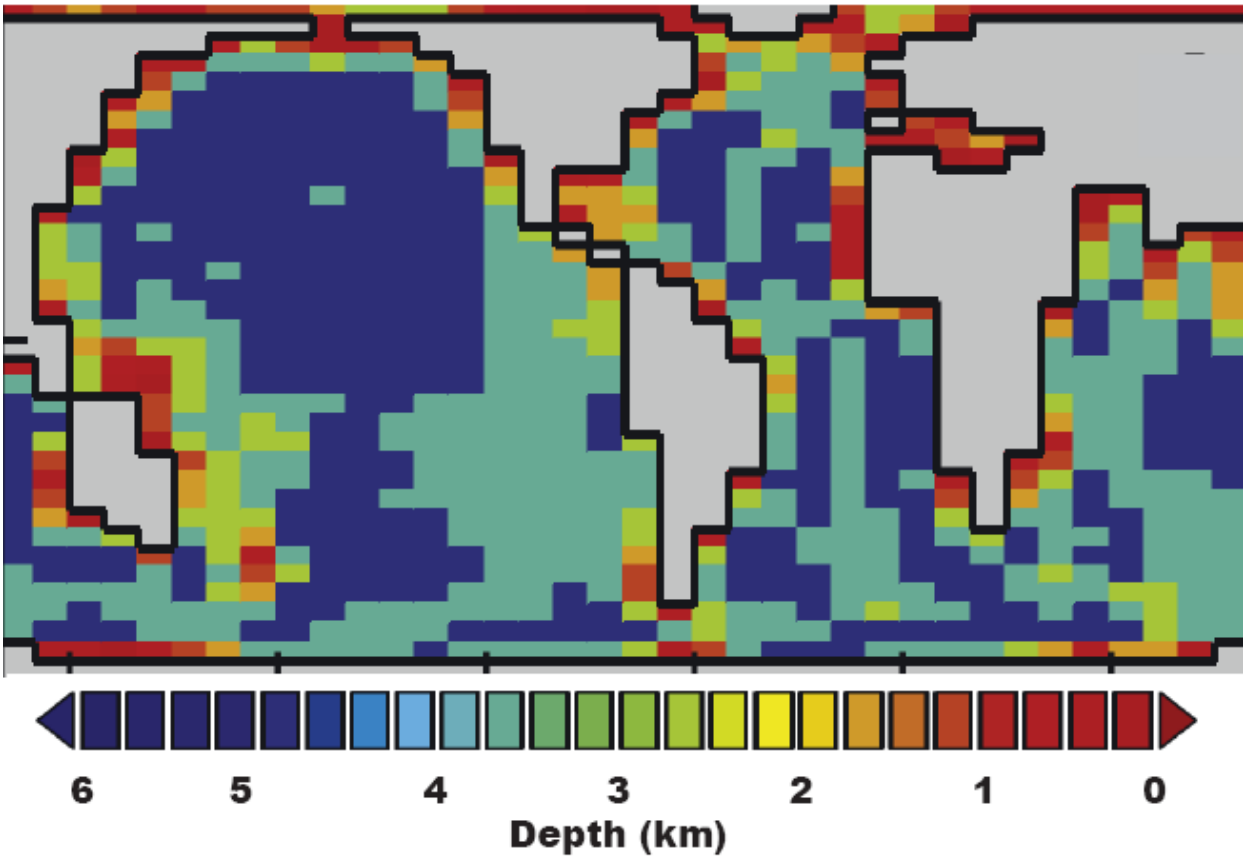

For this study, an ensemble of 934 simulated experiments was conducted in which 36.7 Gt of liquefied CO_2 was injected into every ocean grid cell over a one-year period. For comparison, the annual global emissions for power generation are 10 Gt CO_2/y [*Center for Global Development*, 2007]. Realistic amounts of CO_2 that could be used for ocean carbon injection will be substantially smaller even than these global emissions estimates, due to the difficulties associated with consolidating large amounts of liquefied CO_2 in one location. The amount of 36.7 Gt CO_2 was chosen for this study because this amount is large enough to be traceable within the ocean model simulations over the 1000-year timescale, but is small enough that it does not overwhelm the calculations of carbonate chemistry within the model. For each experiment, the injected CO_2 was treated as a tracer that was circulated via the BIOGEochemical Model (BIOGEM) component of GENIE-1 (Figure 5). BIOGEM calculates the redistribution of tracer concentrations in each grid cell of the ocean. In each of these experiments, the fate of the CO_2 was then monitored at several time periods (i.e., 10, 50, 100, 200, 500, and 1,000 years) in order to estimate the fraction of injected CO_2 that had 'leaked' to the atmosphere.

Several experimental scenarios were designed to examine the fate of injected liquefied CO_2 (Table 1). First, injected CO_2 was monitored in two different climate scenarios: the first without any anthropogenic induced atmospheric CO_2 change (NO-CLIMATE-CHANGE), and the second with three times the radiative forcing than that of preindustrial levels, in which the Atlantic Meridional Overturning Circulation (AMOC) has collapsed (WARMER-CLIMATE). The AMOC is a large heat transportation system and has major impacts on the northern hemisphere climate (Figure 7). Paleoclimatic evidence suggests that this circulation system has been quite different from that of today during past geologic time periods, and that changes in the AMOC can occur rather abruptly over the course of decades [*Lynch-Stieglitz et al.,* 2007]. The purpose of this second experiment was to examine what might happen to the injected CO_2 in the case of extreme climate change, where ocean circulation is altered dramatically. All scenarios held atmospheric CO_2 concentrations constant at a pre-industrial level of 278 ppm to better isolate the impacts of climate-induced changes in ocean circulation. For example, in the WARMER-CLIMATE scenario, only the radiative forcing was changed, not the

background atmospheric CO_2 concentrations. Had both the background CO_2 concentrations and the radiative forcing been changed, it would have been difficult to determine which variable caused the change in relative efficiency at each site.

Table 1. Liquefied CO_2 injection experiments using GENIE-1

Scenario Name	**Description**
CONTROL 1	Atmospheric pCO_2 held constant at 278 ppm.
CONTROL 2	36.7 Gt CO_2 injected into pre-industrial (i.e. pCO_2 = 278 ppm) atmosphere
NO-CLIMATE-CHANGE	36.7 Gt CO_2 injected into every ocean grid cell; atmospheric pCO_2 held constant at 278 ppm
WARMER-CLIMATE	36.7 Gt CO_2 injected into every ocean grid cell; 3x radiative forcing imposed such that Atlantic Meridional Overturning Circulation is collapsed in year 1; atmospheric pCO_2 held constant at 278ppm
SEDIMENT-INTERACTION	36.7 Gt CO_2 injected into every ocean grid cell; injection includes deep-sea $CaCO_3$ sediment interaction; atmospheric CO_2 held constant at 278 ppm
BUFFERED-CO_2	36.7 Gt CO_2 injected into every ocean grid cell; CO_2 injected as 2x Dissolved Inorganic Carbon (DIC) +2x Alkalinity (ALK) to emulate pre-reaction of CO_2 with $CaCO_3$; atmospheric CO_2 held constant at 278 ppm

Figure 7. Schematic drawing of the current configuration of the Atlantic Meridional Overturning Circulation [taken from *NSIDC*, 2009]

Red arrows represent relatively warm water from lower latitudes, while blue arrows represent relatively cooler water, which sinks in the North Atlantic regions before being transported throughout the rest of the ocean. The AMOC is the source of relatively young ventilation ages (~300 years) in the North Atlantic Basin, while North Pacific deep waters at the end of the circulation system have remained isolated from the surface for much longer time periods (on the order of 1,000 years). White regions show the average area covered by sea ice.

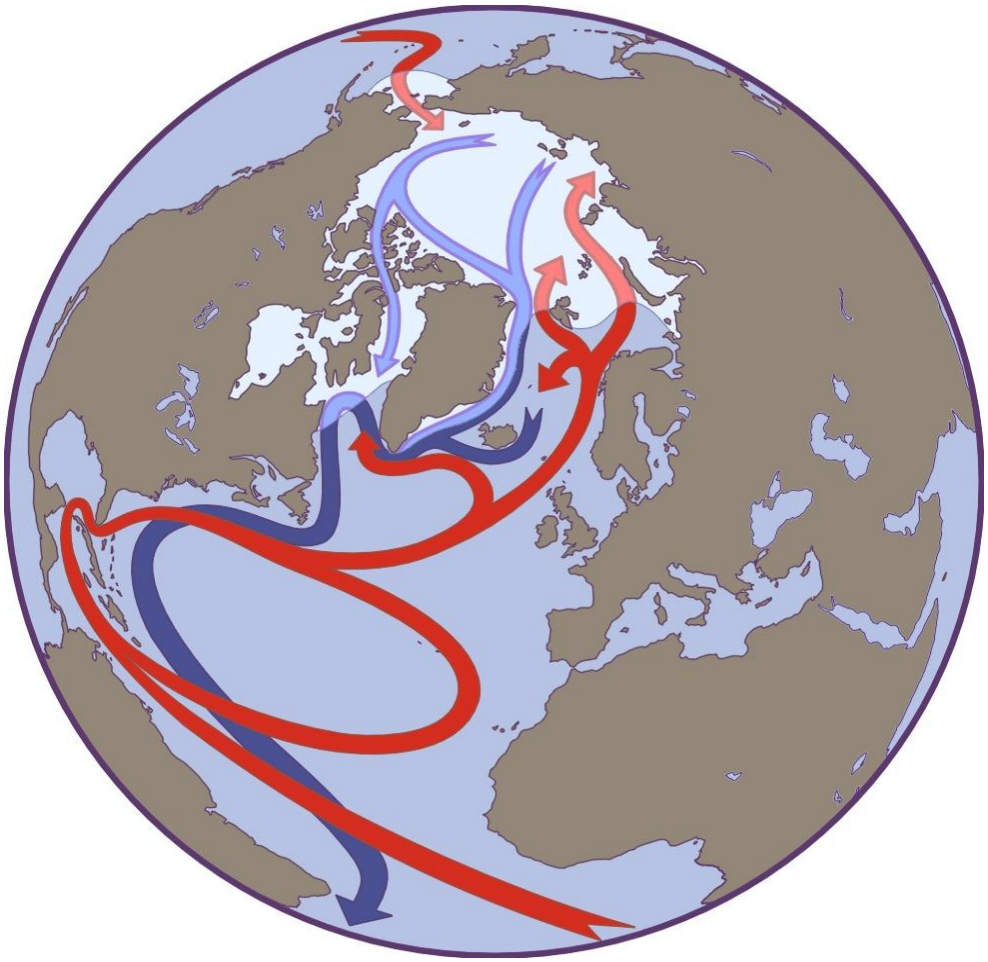

Sediments on the sea-floor help to buffer the acidification of seawater caused by CO_2 addition. This buffering is provided by the natural dissolution of carbonate ($CaCO_3$) minerals that aid in storing more CO_2 from the atmosphere with less change in ocean pH [*Archer et al.*, 1998] (Appendix A). To examine the impact of buffering from $CaCO_3$ minerals on the injected CO_2, two additional simulations were done. The first

(SEDIMENT-INTERACTION) investigated the effects of interactions between $CaCO_3$ sediments and the liquefied CO_2. To simulate this interaction, the deep–sea sediment module (SEDGEM) was added to GENIE-1 (Figure 5). SEDGEM calculates the net accumulation/dissolution of $CaCO_3$ at the surface sediment layer and the stack of sediment storage layers underneath, as well as the mixing between these layers caused by bioturbation [*Ridgwell and Hargreaves,* 2007]. In the second experiment (BUFFERED-CO_2), the liquefied CO_2 was buffered by the inclusion of a $CaCO_3$ 'buffer' at the time of injection. Because most Dissolved Inorganic Carbon (DIC) is in the form of HCO_3^- in the ocean (Appendix A), the main effect of dissolving $CaCO_3$ in seawater at the time of liquefied CO_2 addition is to shift CO_2 from the atmosphere to the oceans in equilibrium, buffering the effect of CO_2 on pH [*Golomb and Angelopoulos,* 2001] [1].

$$CaCO_3\,(s) + CO_2\,(g) + H_2O \leftrightarrow Ca^{2+} + 2HCO_3^- \qquad [1]$$

Since adding CO_2 to seawater increases only DIC and buffering CO_2 with $CaCO_3$ increases both DIC and Total Alkalinity (ALK), the BUFFERED CO_2 scenario was emulated by doubling both DIC and ALK.

Two control experiments were also run for 1,000 years. The first control experiment (CONTROL 1) was a simulation in which atmospheric CO_2 was held constant at 278 ppm and no additional CO_2 was added to the ocean or atmosphere. In CONTROL 2, 36.7 Gt CO_2 was added to the atmosphere in order to estimate what fraction of this CO_2 would enter the ocean via natural air-sea gas exchange processes.

For each time period and at each grid cell, one can calculate the fraction of the total mass of CO_2 that has remained in the ocean, divided by the total mass of CO_2 that was originally injected. This calculation provides an estimate of the "absolute efficiency," which has been used in previous studies [*Orr*, 2004, *Caldeira and Wickett,* 2005]. In this study, *relative efficiency*, or the fraction of total mass of injected CO_2 that has remained in the ocean relative to what fraction of this CO_2 would wind up in the ocean via natural air-sea gas exchange processes (CONTROL 2), was estimated. I estimate relative efficiency (RE_{GRIDi}) of injection at each grid cell *i* in the following manner:

$$RE_{GRIDi}\ (\%) = \frac{\left[(pCO2_{CONTROL2})_t - (pCO2_{GRIDi})_t\right]}{\left[(pCO2_{CONTROL2})_t - (278\,ppm)\right]} * 100 \qquad [2]$$

where $(pCO2_{CONTROL2})_t$ is the concentration of carbon dioxide in the atmosphere in the CONTROL 2 experiment at time *t* and $(pCO2_{GRIDi})_t$ is the concentration of CO_2 in the atmosphere following CO_2 injection into any given grid cell *GRIDi* at time *t*. The numerator of this equation estimates difference in atmospheric pCO_2 between the CONTROL 2 and each of our grid cell injection experiments. In other words, the numerator describes how much lower atmospheric pCO_2 is due to ocean injection at one particular location in the ocean, when compared to the control simulation where the same amount of carbon is injected into the atmosphere. The denominator represents the difference between the pre-industrial atmospheric CO_2 concentrations (e.g., 278 ppm) and the atmospheric CO_2 concentration following the injection of 36.7 Pg CO_2 directly into the atmosphere at time *t*. At year 0, the denominator would equal 36.7 Pg CO_2 (or 281.4 – 278 = 3.4 ppm). Figure 8 demonstrates how absolute and relative efficiencies are calculated for an injection at a sample grid cell, in this case, site AG15 off the coast of Yemen and Oman and site I4 off the coast of Kamchatka.

Figure 8. Depiction of relative and absolute efficiencies (%) over the 1,000 year model run for site AG15 (off the coast of Yemen and Oman) and I4 (off the coast of Kamchatka), for the NO-CLIMATE-CHANGE scenario

The top panel (a) depicts changes in atmospheric pCO_2 (ppm) for CONTROL 1 (dashed red), CONTROL 2 (solid red), site I4 (blue), and site AG15 (orange), in the NO-CLIMATE-CHANGE scenario. In the CONTROL 1 simulation, atmospheric pCO_2 is held constant at pre-industrial levels (i.e. pCO_2 = 278 ppm). In the CONTROL 2 experiment, 36.7 Gt CO_2 is injected directly into the pre-industrial (i.e. pCO_2 = 278 ppm) atmosphere at year 0. The bottom panel (b) shows absolute (dashed) and relative (solid) efficiencies for site I4 (blue) and site AG15 (orange line). Absolute efficiency is the total mass of CO_2 that has remained in the ocean divided by the total mass of CO_2 that was originally injected (36.7 Gt CO_2). Relative efficiency represents the fraction of total mass of CO_2 that has remained in the ocean relative to what fraction of this CO_2 would wind up in the ocean via natural air-sea gas exchange processes (CONTROL 2), as calculated using equation [2] in the text.

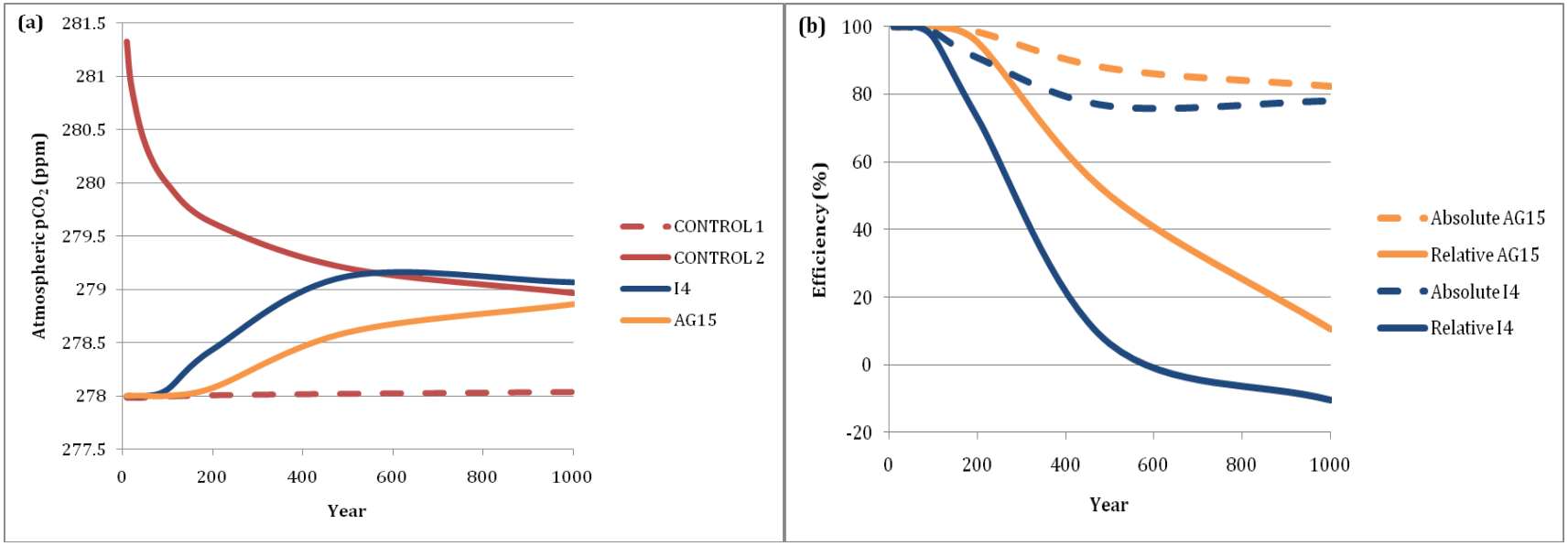

Incorporating relative efficiency permits an estimate of how much of the liquid CO_2 injection would actually reduce atmospheric CO_2 compared to what would have occurred naturally via air-sea gas exchange processes. Interestingly, this definition of relative efficiency allows for cases in which relative efficiencies become negative. Negative efficiencies can result any time that atmospheric pCO_2 in the ocean injection experiments $(pCO2_{GRIDi})_t$ are greater than the atmospheric pCO_2 in the CONTROL 2 experiment $(pCO2_{CONTROL2})_t$ in which CO_2 is injected directly into the atmosphere and allowed to invade the ocean naturally.

2.2 Filtering Criteria

While these Earth System model simulations provide a first-order analysis of which sites will be physically most efficient at sequestering injected CO_2, one must consider more than just physical efficiency when choosing suitable sites for large-scale geo-engineering projects. Choosing suitable sites must ultimately satisfy multiple sets of objectives, including objectives dealing with public safety, environmental health, societal values and economic costs. In the past, Multi-Attribute Utility Analysis (MAUA) methods have been used to deal with similar environmental problems such as determining sites for disposal of nuclear and other hazardous waste. For example, a MAUA was used to demonstrate that the proposed underground repository for nuclear waste storage at Yucca Mountain would be inferior to other strategies such as temporary above ground storage. In this case, MAUA estimated that the proposed Yucca Mountain facility would cost the equivalent of US$10 to $50 billion more than other options [*Keeney and von Winterfeldt*, 1994]. MAUA approaches work by using stakeholders to establish which criteria are most relevant for site selection based on specified management objectives, and allowing them to assign attributes (i.e., weightings) to each criterion in order to provide a score for each proposed location. Ultimately, the calculated scores for each potential site are used to select optimal locations. The advantage of the MAUA approach is that it can systematically consider a broad range of perspectives in site selection, and that decision makers have the ability to apply additional weight to criteria are more important than others when selecting sites. Furthermore, the method is easily understandable, flexible,

and transparent, and it does not depend on the technical expertise of the participants [*Gough and Shackley*, 2006].

The aim of this study is very similar to that of a typical MAUA in that the goal is to focus on site selection for potential ocean CO_2 injection based on a series of criteria that take into account certain broader socio-environmental and technological constraints that are likely to provide practical limits to the use of this mitigation technology. Table 2 displays a sequence of filtering criteria used to distill a selection of suitable injection sites. The physical criteria account for limitations of physical chemistry that prevent CO_2 from sinking in the ocean. Technological criteria account for the limits of technology by considering only locations that can be reached by the longest and deepest pipelines in use today. Socio-environmental criteria limit sites based on their previous and proposed designation as Marine Protected Areas (MPAs) (Appendix B). MPAs cover a wide range of designations that have been identified to protect living, non-living, cultural, and/or historical resources. Some notable designations include Wildlife Refuges, Biosphere Reserves and UNESCO World Heritage Sites. Although they vary depending on the type of designation, typical regulations within MPAs include restrictions on fisheries, oil and gas mining, access for tourism, and any sort of development or construction. MPAs are located in the territorial waters of coastal states, where enforcement of these restrictions can be ensured [*UNEP-WCMC*, 2008]. MPAs were chosen as the SOCIO-ENVIRONMENTAL filtering criteria for this study because they represent internationally-recognized and well-defined geographic areas that were designed to achieve specific international socio-environmental conservation objectives.

Table 2. Filtering criteria and filter combinations

Filter #	Description	Area omitted after filtering*
0	No filter applied	
1	**PHYSICAL A** - omits sites shallower than 800 m, based on understanding that liquefied CO_2 injected at depths shallower than 800m may convert from a liquid to gas and form a plume that could erupt [*Zhang,* 2005]	z < 800 m
2	**PHYSICAL B** - omits all sites shallower than 3,000m, based on knowledge that liquid CO_2 becomes denser than seawater and sinks to bottom at depths greater than 3,000m [e.g., *IPCC,* 2005]	z < 3,000 m
3	**TECHNOLOGICAL A** – omits any site deeper than 2,500m, based on the current technological pressure threshold for deep-sea pipelines [*Statoil*]. Additional engineering advancements would be necessary to place pipelines below this depth	z >2,500 m
4	**TECHNOLOGICAL B** - omits sites further than 1,166 km off coast, based on the current technological limit on deep-sea pipeline length [GASSCO, 2008]	distance to coast > 1,166 km
5	**SOCIO-ENVIRONMENTAL**- omits all national and international marine protected areas, including proposed sites that are not yet officially recognized by government but have previously been designated as environmentally important to society (e.g., UNESCO World Heritage Property such as Shark Bay, and National Wildlife Refuges such as the Alaska Maritime National Wildlife Refuge) [*UNEP-WCMC,* 2009] [Appendix B]	marine protected areas
13	**PHYSICAL A & TECHNOLOGICAL A**	z <800 m, z > 2,500 m
25	**PHYSICAL B & SOCIO-ENVIRONMENTAL**	z < 3,000 m, marine protected areas
134	**PHYSICAL A**, **TECHNOLOGICAL A & TECHNOLOGICAL B**	z< 800m, z > 2,500 m, distance to coast < 1,166 km
135	**PHYSICAL A**, **TECHNOLOGICAL A & SOCIO-ENVIRONMENTAL**	z < 800m, z > 2,500 m, marine protected areas
1345	**PHYSICAL A**, **TECHNOLOGICAL A, TECHNOLOGICAL B & SOCIO-ENVIRONMENTAL**	z < 800m, z > 2,500 m, distance to coast >1166km, marine protected areas

*z = ocean depths that are omitted after filtering

Not all of these filtering criteria are independent. For example, PHYSICAL B, which excludes all sites above 3,000 m, contains all sites that are filtered out by criterion

PHYSICAL A, which only excludes sites above 800 m. Furthermore, not all of these filters can be combined iteratively. For example, combining the filter TECHNOLOGICAL A (which excludes all sites *below* 2,500 m) with PHYSICAL B (which excludes all sites *above* 3,000 m) would eliminate every ocean site. For this analysis, I have opted to combine selected filters to generate the most complete picture of sites that are feasible based the given criteria (Table 2). Finally, it is important to note that, unlike typical MAUA approaches, this study does not apply differential weighting to each criterion, but rather gives each criterion equal weight. In other words, if a site does not meet one of the filtering criteria, it is excluded as a possible CO_2 injection site. Furthermore, the aim of this study is not to identify a single "optimal" site location. Instead, this approach identifies the key issues that are likely to be most critical to further development of ocean CO_2 storage.

Another important criterion for evaluating sites that is not included as a filter involves economic cost. Injection of liquefied CO_2 will only become a viable option when it becomes economically competitive, or when society's "willingness to be compensated" for the mitigation of climate change reaches the estimated cost of CO_2 injection. In this analysis, sites are not filtered based on a fixed price criterion (i.e., selecting a monetary value for 'willingness to be compensated' based on personal judgment). Instead, simple first order cost estimates were made based on the distance between potential injection sites and regions of the world where emissions from power plants exceeded 100 Mt CO_2/y.

The total amount of power plant emissions per GENIE-1 site (grid cell) was calculated based on global estimates of annual CO_2 emissions from coal-burning power plants for 2007 [*Center for Global Development,* 2007] (Appendix C). Next, the distance between land sites emitting more than 100 Mt CO_2/y and ocean injection sites that remained after the most comprehensive filtering criteria (1345) was calculated. This distance was then converted to cost per ton of CO_2 using a previously established scaling factor of US$6.20/100 km of pipeline per ton CO_2 stored net stored [*Akai et al.,* 2004]. In the estimate of Akai *et al*. [2004], CO_2 is captured from a coal power plant with a net

generation capacity of 600 Megawatts and transported by CO_2 pipeline for injection at a depth of 3,000 m.

An additional cost of US$13.00/ton (t) CO_2 was considered to account for neutralizing the impact of CO_2 on ocean acidity [*Golomb et al.*, 2007]. The estimate of Golomb *et al*. [2007] includes of the cost of mining approximately 0.5 tons of limestone (mineral $CaCO_3$) for every ton of liquid CO_2 as well as the associated limestone pulverization and shipping costs. Ultimately, the cost per ton CO_2 was converted to cost per ton CO_2 net stored by dividing the cost by the specific % relative efficiency for each site in either the NO-CLIMATE-CHANGE or BUFFERED-CO2 scenario. Because the relative efficiencies of each site decreases with time, the cost per ton of CO_2 stored will also vary depending on the time scale that one requires the CO_2 to be stored. I have chosen to estimate the cost per net ton of CO_2 stored for year 100, with the assumption that this mitigation option is likely to be used as a temporary measure to slow down the impacts of anthropogenic climate change over the course of one century, to provide time for other mitigation options to be pursued.

The distance between the centers of two grid cells, which are approximately 5,556 km^2 in area, is estimated. Thus, cost estimates, which are based on distance, incorporate some degree of uncertainty because the actual distances between injection and emission sites could be anywhere within these grid cells. To account for these errors, distances between the two closest and furthest grid corners between injection and emission sites are also included.

3 RESULTS

3.1 Relative Efficiency of Injection Sites

After 200 years in the NO-CLIMATE-CHANGE scenario, the open ocean sites (sites not bordering a coastline) have an average relative efficiency of 94% (Figure 9d). On average, the coastal sites (i.e., all grid cells that directly share a coastline) still have relative efficiencies of 65% at year 200. The average relative efficiency is reduced to 15% by year 1,000 at the coastal sites (Figure 9d, e). The most efficient region of the ocean, with an average relative efficiency of 70% after 1000 years, is the central North Pacific Ocean (8-36ºN, 140-160ºW; Figure 9f). On the timescale of zero to 50 years, relative efficiencies remain greater than 95% in all open ocean locations. In contrast, some coastal sites already possess negative relative efficiencies by year 50 (Figure 9b). As stated previously, a negative relative efficiency can occur when ocean injection at a particular location actually results in *higher* atmospheric CO_2 concentrations than if CO_2 had simply been released straight into the atmosphere.

Figure 9. Relative CO_2 sequestration efficiencies (%) for each location for the NO-CLIMATE-CHANGE scenario

36.7 Gt CO_2 was injected into each grid cell and % relative efficiencies are shown for years (a) 10, (b) 50, (c) 100, (d) 200, (e) 500 and (f) 1,000.

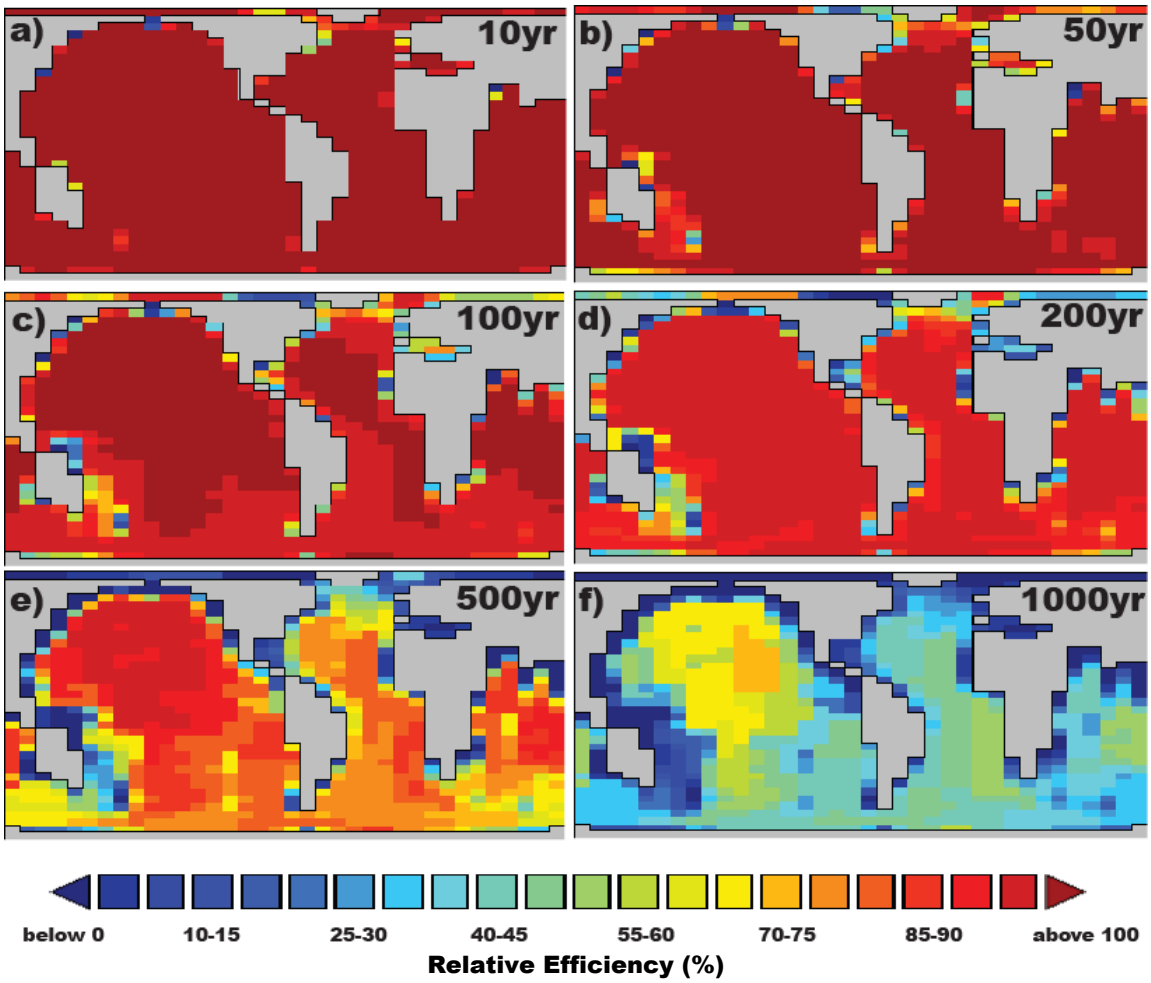

Following 200 years in the WARMER-CLIMATE scenario, virtually the same average relative efficiencies are evident in the open ocean (94%) and coastal sites (64%) when compared to the NO-CLIMATE-CHANGE scenario. However, in contrast with the NO-CLIMATE-CHANGE scenario, after 1,000 years the most efficient sites for injecting liquefied CO_2 are found in the central North Atlantic Ocean (11-28ºN, 20-40ºW, Figure 10f). While the most efficient site locations have changed, there is little difference (<4%) in relative efficiency between each site when comparing the WARMER CLIMATE and the NO-CLIMATE-CHANGE scenarios throughout all the time periods (0-1,000 years).

Figure 10. Relative ocean CO_2 sequestration efficiencies (%) for each location for the WARMER-CLIMATE scenario

36.7 Gt CO_2 was injected into each grid cell and % relative efficiencies are shown for years (a) 10, (b) 50, (c) 100, (d) 200, (e) 500 and (f) 1,000.

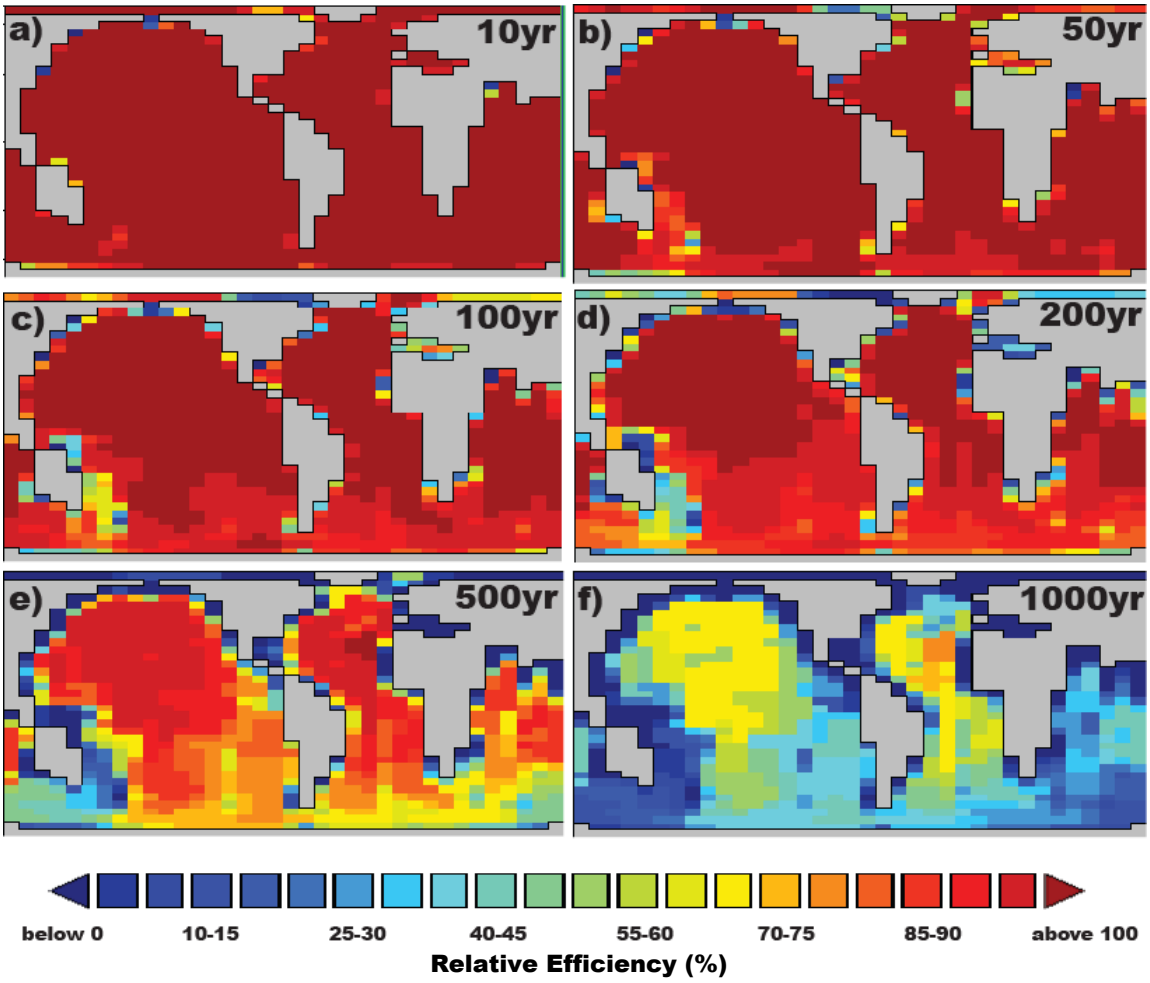

Very little difference (<5%) in relative efficiencies exists between the SEDIMENT-INTERACTION and NO-CLIMATE-CHANGE scenarios for all open ocean sites, on a site-by-site basis, over any time period. The coastal sites have the same average relative efficiency (65%) by year 200 in both scenarios. However, by year 1,000, the average relative efficiency for all coastal ocean sites in the SEDIMENT-INTERACTION scenario is reduced to 10% relative efficiency (approximately 5% less than coastal sites in the NO-CLIMATE-CHANGE scenario).

In the BUFFERED-CO_2 scenario, relative efficiencies are higher at all sites and for every time period than in scenarios where CO_2 is not buffered (Figure 11a-f). After 200 years, average relative efficiencies of 98% and 88% are found at open ocean and coastal sites, respectively (Figure 11d). By year 1,000, the average relative efficiency is 80% for open ocean sites and 72% for coastal sites (Figure 11f). Not one injection site has a relative efficiency below 64%. The most efficient region of the ocean, retaining an average of 88% relative efficiency at year 1,000, is the central North Pacific Ocean (8º-40ºN, 120-180ºW; Figure 11f). This region is similar to that seen in the unbuffered, NO-CLIMATE-CHANGE scenario, although the area of highest relative efficiency is much larger and the overall relative efficiencies are higher. In contrast to all three other scenarios, not one site in the BUFFERED-CO_2 scenario possesses a negative relative efficiency in year 1,000.

Figure 11. Relative ocean CO_2 sequestration efficiency (%) at each location for the BUFFERED-CO_2 scenario

36.7 Gt CO_2 was injected into each grid cell and percent efficiencies are shown for years (a) 10, (b) 50, (c) 100, (d) 200, (e) 500 and (f) 1,000.

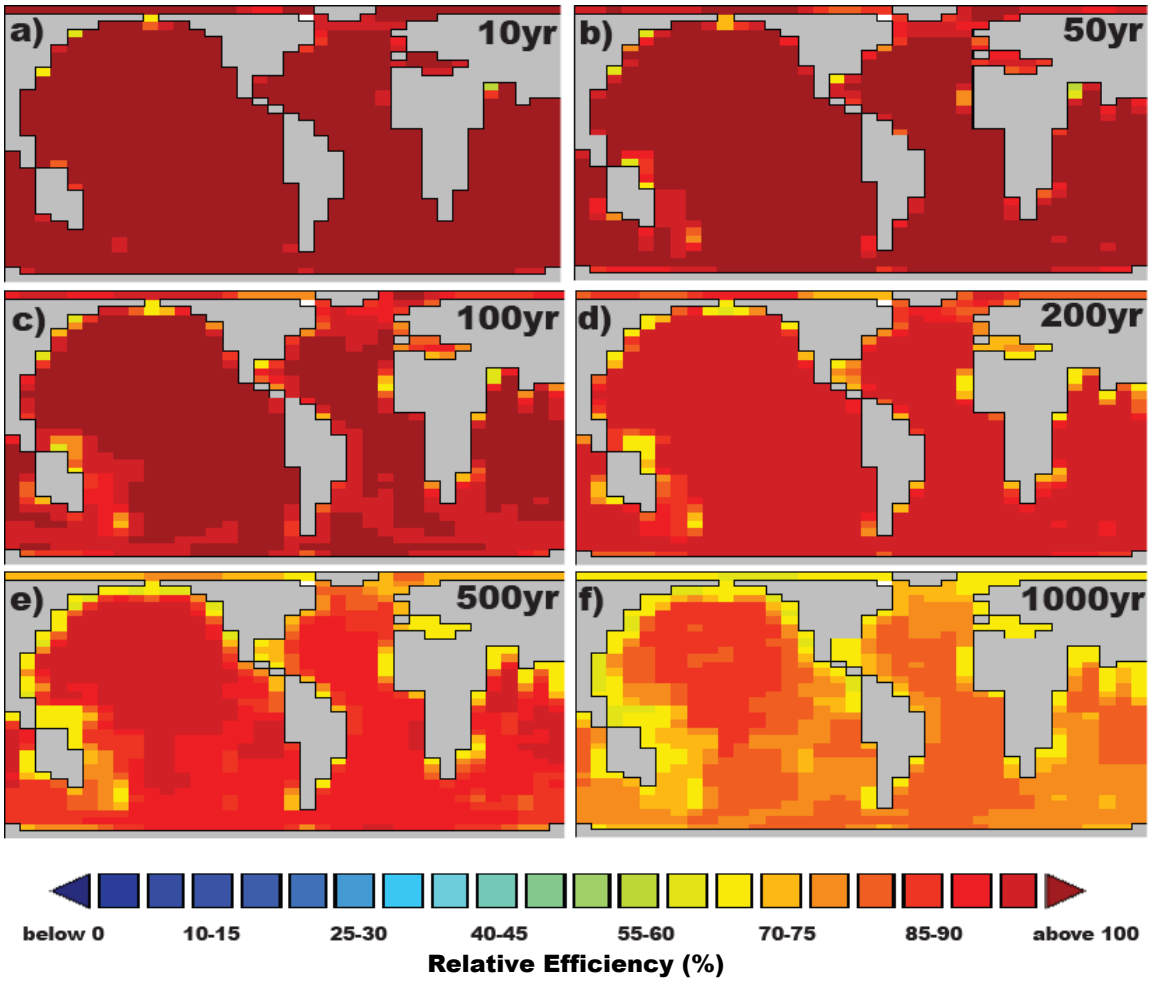

3.2 Relative Efficiency of Selected Sites after Filtering Criteria are Applied

Application of the filtering criteria identifies sites that are most likely usable for CO_2 injection, but this process also tends to eliminate high-efficiency sites in the open ocean (Figure 12). Once the most comprehensive filter (1345) is applied, only 46 sites remain, 27 of which exist in high latitude regions (i.e., poleward of 62.7º). Since GENIE-1 does not effectively replicate observed values of anthropogenic CO_2 uptake by the ocean at the high latitudes due to the lack of observed data [*Ridgwell et al.,* 2007], this analysis focused on the remaining 19 sites, which hereafter will be referred to as the selected sites (Figure 12j).

Figure 12. Filtering criteria applied to all sites, for year 100 in the NO-CLIMATE-CHANGE scenario

Filtering criteria are a) 0, b) 1, C) 2, d) 4, e) 5, f) 13, g) 25, h) 134, i) 135, j) 1345. See Table 2 for definition of filtering criteria.

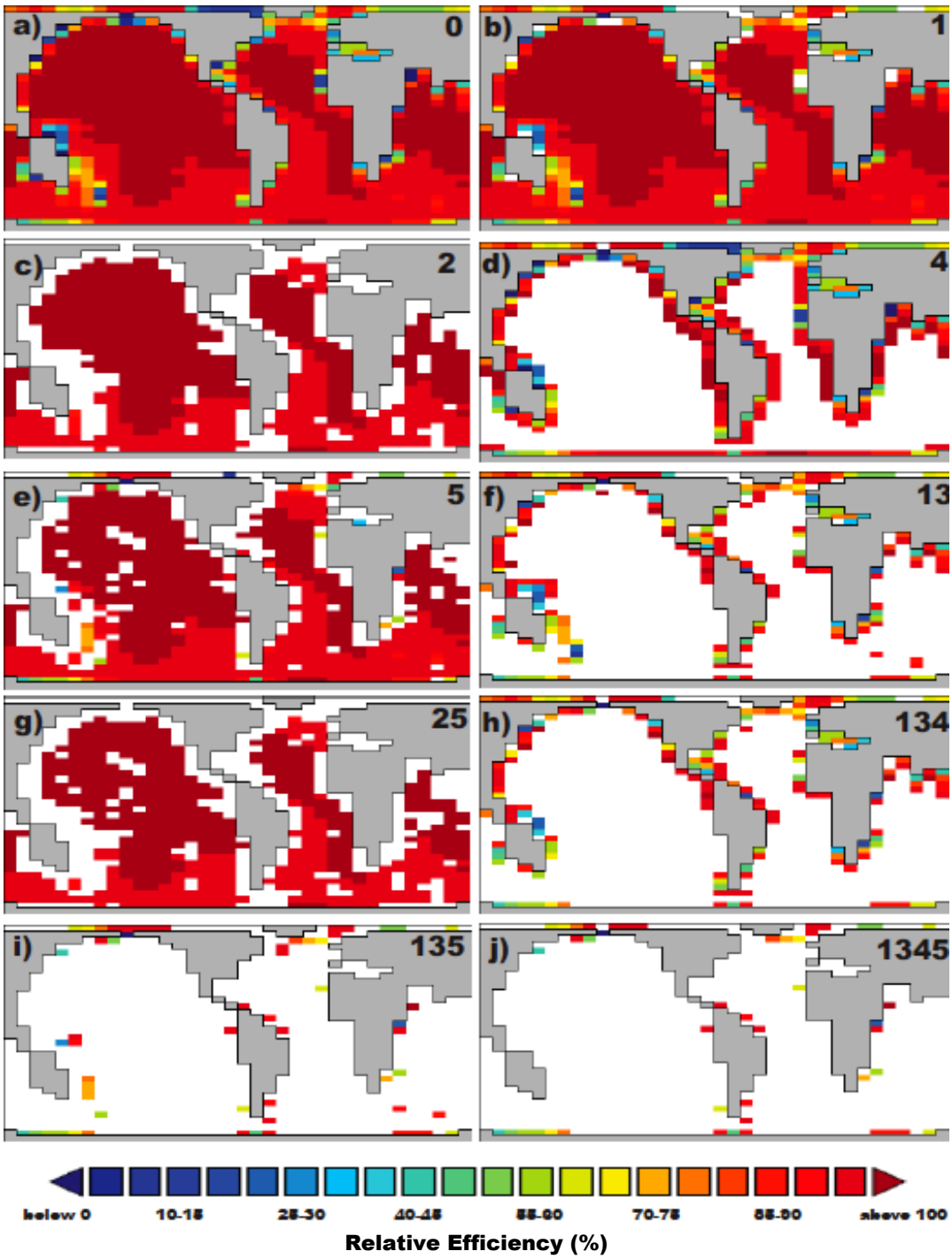

After 200 years in the NO-CLIMATE-CHANGE scenario, the relative efficiencies of the 19 selected sites range from 1% (off the coast of Somalia) to 95% (off the coast of Yemen and Oman). After 1,000 years, only 13 of these sites possess a positive relative efficiency, ranging from 1% (off the coast of Yemen and Oman) to 9% (off the coast of Mozambique) (Figure 13a). In the WARMER-CLIMATE scenario, the selected sites have an average relative efficiency of 65% after 200 years, with values ranging from 6% (off the coast of Somalia) to 97% (off the coast of Yemen and Oman). After 1,000 years, 8 sites have positive relative efficiencies, ranging from 1% (off the coast of Chile) to 30% (off the coast of the Falkland Islands), with an average of 11% (Figure 13b). The SEDIMENT-INTERACTION scenario shows the same average relative efficiency (65%) as the NO-CLIMATE-CHANGE scenario after 200 years. Yet after 1,000 years, this scenario only has 5 sites that possess a positive relative efficiency, ranging from 3% (off the coast of Greenland) to 34% (off the coast of the Falkland Islands) (Figure 13c). Following 200 years in the BUFFERED-CO_2 scenario, the selected 19 sites have an average relative efficiency of 87%. By year 1,000, all 19 sites still have positive relative efficiencies ranging from 64% (off the east coast of Kamchatka) to 79% (off the coast of the Falkland Islands) (Figure 13d). On the timescale of zero to 50 years, very little difference (<7%) is found between the average relative efficiencies for each scenario.

Figure 13. Relative efficiency of 19 selected sites found between latitudes 62.7ºN and 62.7ºS, following the application of filtering criteria 1345, at year 1,000 for scenarios (a) NO-CLIMATE-CHANGE, (b) WARMER-CLIMATE, (c) SEDIMENT-INTERACTION, (d) BUFFERED CO_2

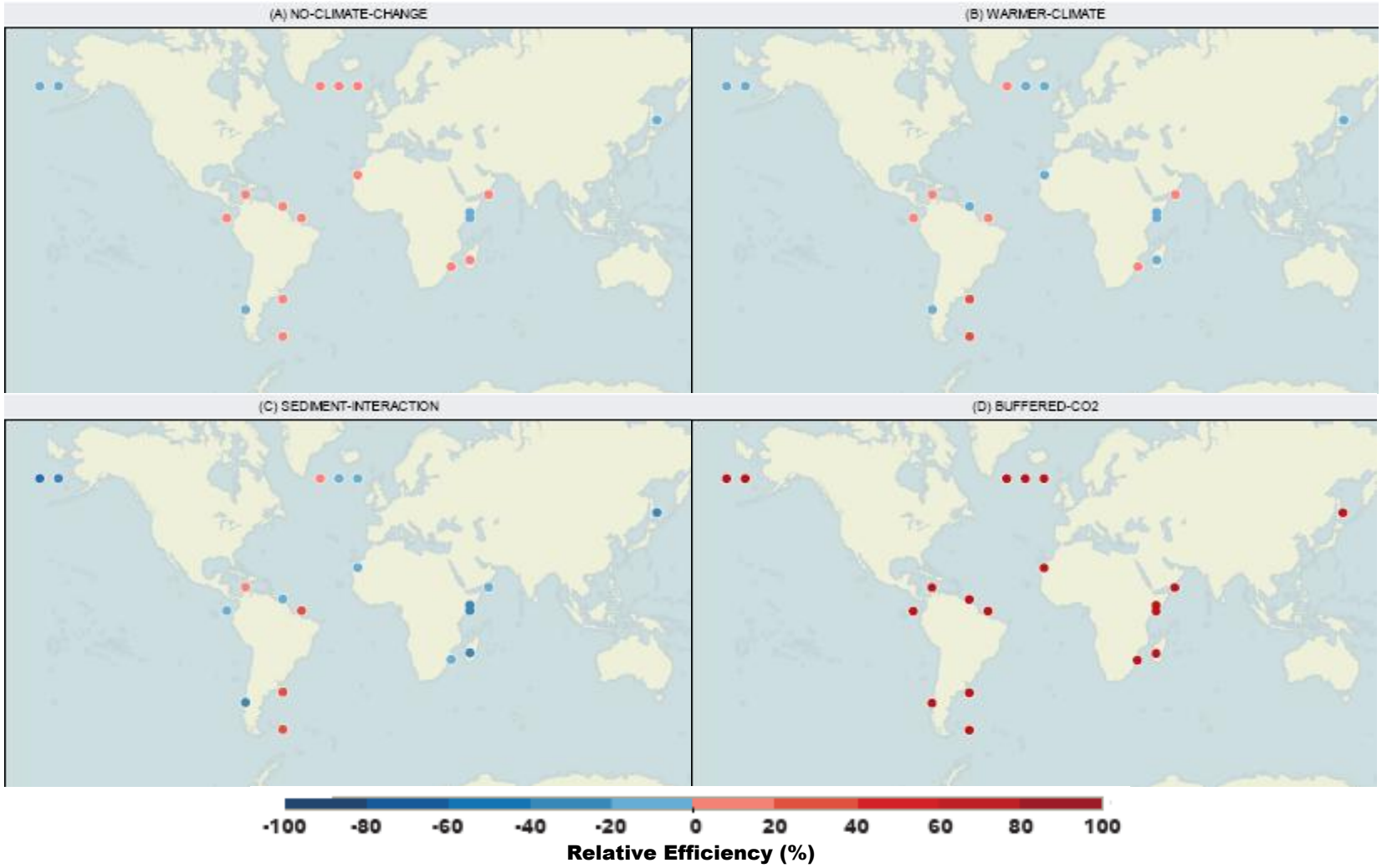
(A) NO-CLIMATE-CHANGE
(B) WARMER-CLIMATE
(C) SEDIMENT-INTERACTION
(D) BUFFERED-CO2
-100
-80
-60
-40
-20
0
20
40
60
80
100
Relative Efficiency (%)

3.3 Estimated Costs of Reaching Selected Injection Sites from Regions of Greatest Annual CO_2 Emissions

Once power plant emissions data are summed for every grid location in GENIE-1, only 30 sites emit greater than 100 Mt/CO_2 annually. The majority of these sites are located in eastern Asia and the eastern United States (Figure 14a, c), although substantial emissions are also found in Europe and southern Africa.

Figure 14. Locations of highest densities of CO_2 emitting power plants (red dots), estimated by summing total emissions per GENIE-1 grid cell, and potential injection sites (blue dots)

(a) Grid cells where total power plant emissions are >100 Mt CO_2/y; remaining injection sites after applying 1345 filtering criteria (b) Grid cells where total power plant emissions are >50 Mt CO_2/y; remaining sites after 1345 filtering criteria, (c) Grid cells where total power plant emissions are >100 Mt CO_2/y; remaining sites after 134 filtering criteria, (d) Grid cells where total power plant emissions are >50 Mt CO_2/y; remaining sites after 134 filtering criteria. Annual power plant emissions data is from the Center for Global Development [2007]. Color scale represents total amount of CO_2 emitted (Mt) at each location. Light blue dots in (c) and (d) represent locations with both high densities of CO_2-emitting power plants and a potential injection site. Yellow dots represent the seven sites in the Orr [2004] study.]

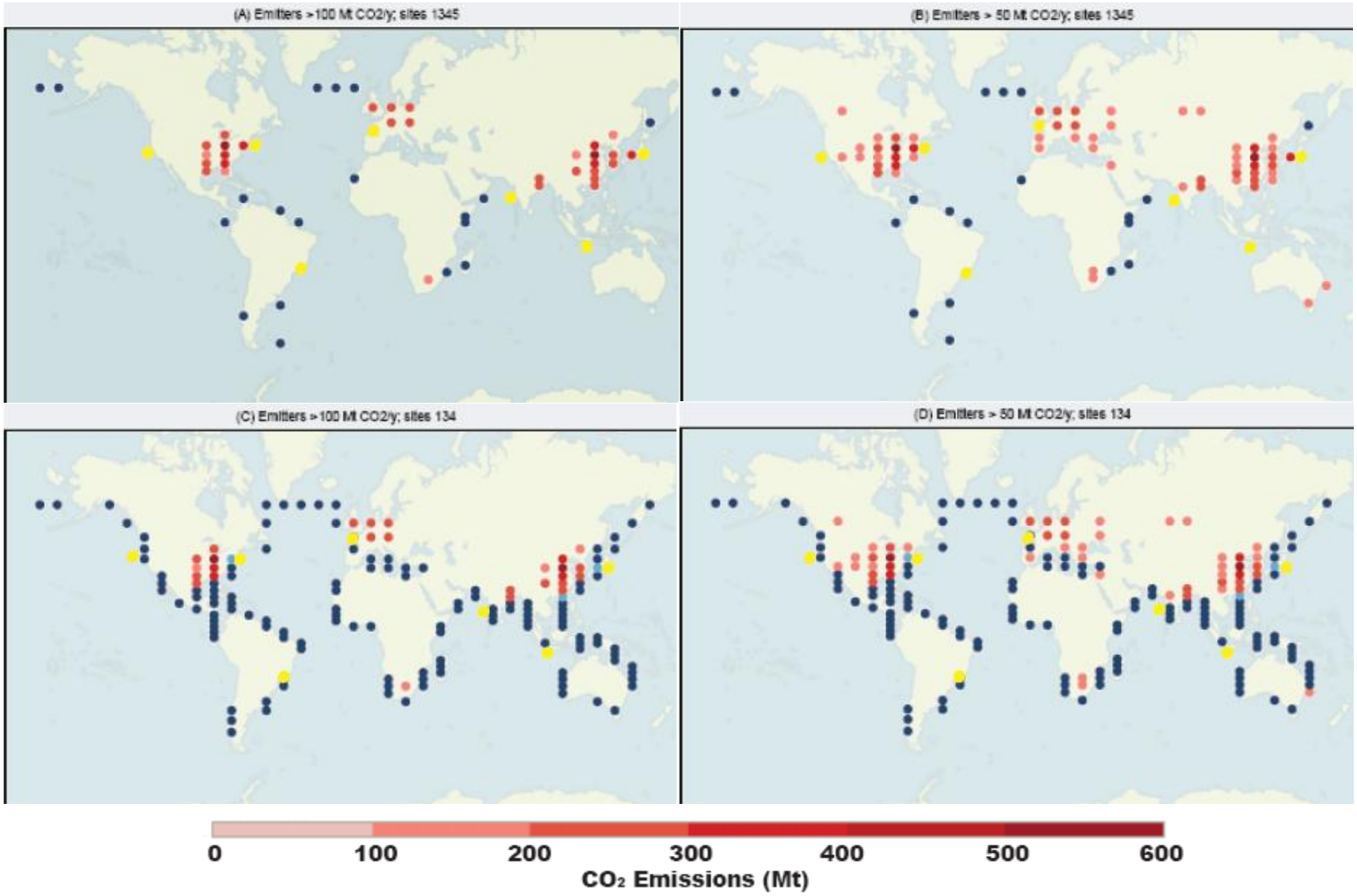
(A) Emitters >100 Mt CO2/y; sites 1345
(B) Emitters > 50 Mt CO2/y; sites 1345
(C) Emitters >100 Mt CO2/y; sites 134
(D) Emitters > 50 Mt CO2/y; sites 134
0
100
200
300
400
500
600
CO₂ Emissions (Mt)

The distances between the 19 selected sites and the closest of these 30 high emitting sites range from 887 +1757-887 km to 8169 ± 1482 km (Table 3). Site Z4 off the coast of Scotland (59.55ºN, 15ºW) is the selected site closest to a region with high CO_2 emissions from power plants (site AA5 of England/Ireland (53.75ºN, 5ºW)). This selected injection site has relative efficiencies of 79%, 46%, and 6% at years 50, 200, and 1,000, respectively, in the NO-CLIMATE-CHANGE scenario. In contrast, the selected ocean injection site that is furthest from any region of high emissions is site V34 off the coast of the Falkland Islands (53ºS, 55ºW) which is 9560 ± 1482 km from site S11 of Florida (28.2ºN, 85ºW). Furthermore, only two locations (Z4 off the coast of Scotland and AE27 off the coast of Mozambique) are within 1,166 km of a major emitting region (with current technology, 1,166 km is the maximum length for an ocean CO_2 pipeline).

Table 3. Cost (per ton of CO_2 net stored) estimated to transport and inject CO_2 at the 19 selected sites

Cost is calculated by applying a scaling factor, and in the case of adding carbonate buffer a scaling factor plus an additional cost, to the distance between the injection site and the nearest high CO_2 emitting site and dividing that cost by the specific % relative efficiency for that site in either the NO-CLIMATE-CHANGE or BUFFERED-CO_2 scenario. The location of the center of each grid cell is shown for reference. Relative efficiency in NO-CLIMATE-CHANGE and BUFFERED-CO_2 scenarios are also shown for year 100.

Selected Site ID	Region (off coast of nearest country or state)	Center of Selected Site	Closest High Emissions site ID	Region (nearest country or state)	Center of Closest High Emission Site±	Distance between Selected site and Closest High Emissions Site (km)	Cost (US$/t CO_2net stored)	Relative Efficiency (%) in NO-CLIMATE-CHANGE Scenario	Cost (US$/t CO_2net stored) with Carbonate Buffer	Relative Efficiency (%) in BUFFERED-CO_2 Scenario
Z4	Scotland	48.65°N, 14°E	AA5	England/ Ireland	53.7°N, 5°W	887 +1757 -887	82.06 +162.59 -82.06	67	75.55 +135.48 -75.55	90
AE27	Mozambique	24.65°S, 35°E	AD28	South Africa	28.2°S, 25°E	1071 +2138 -1071	89.73 +179.13 -89.73	74	85.31 +156.51 -85.31	93
T15	Columbia	14.45°N, 75°W	S11	Florida	28.2°N, 85°W	1845 ± 1664	115.55 ± 104.21	99	127.39 ± 103.17	100
Y4	Iceland	59.55°N, 25°E	AA5	England/ Ireland	53.7°N, 5°W	1375 +1585 -1357	116.78 +134.53 -116.78	73	106.79 +120.95 -106.79	92
X4	Greenland	59.55°N, 35°E	AA5	England/ Ireland	53.7°N, 5°W	1924 ± 1464	145.47 ± 110.69	82	139.25 ± 109.23	95
S19	Ecuador	1.6°N, 85°W	S11	Florida	28.2°N, 85°W	2958 ± 920	183.40 ± 57.04	100	196.40 ± 57.04	100

Selected Site ID	Region (off coast of nearest country or state)	Center of Selected Site	Closest High Emissions site ID	Region (nearest country or state)	Center of Closest High Emission Site±	Distance between Selected site and Closest High Emissions Site (km)	Cost (US$/t CO_2net stored)	Relative Efficiency (%) in NO-CLIMATE-CHANGE Scenario	Cost (US$/t CO_2net stored) with Carbonate Buffer	Relative Efficiency (%) in BUFFERED-CO_2 Scenario
AG15	Yemen/ Oman	14.45°N, 55°E	AJ13	India	21.2°N, 85°E	3257 ± 2219	201.93 ± 137.58	100	214.93 ± 137.58	100
AF26	Madagascar	21.2°S, 45°E	AD28	South Africa	28.2°S, 25°E	2162 ± 1244	235.16 ± 135.31	57	167.09 ± 102.42	88
I4	Kamchatka	59.55°N, 175°E	D7	China	44°N, 125°E	3773 ± 1522	241.16 ± 97.28	97	$249.42 ± 108.45	99
F6	Japan	48.65°N, 145°E	E9	Japan	35.7°N, 135°E	1656 ± 1576	244.46 ± 232.64	42	144.59 ±138.16	80
AF19	Somalia	1.6°N, 45°E	AD28	South Africa	28.2°S, 25°E	3942 ± 1753	254.59 ± 113.21	96	258.13 ± 122.92	99
V17	Suriname	8°N, 55°W	S11	Florida	28.2°N, 85°W	3865 ± 2118	254.93 ± 139.70	94	257.79 ± 147.26	98
Z12	Mauritania	24.65°N, 15°W	AB6	France	48.65°N, 5°E	3189 ± 1687	313.84 ± 166.02	63	239.45 ± 133.63	88
W19	Brazil	1.6°N, 45°W	S11	Florida	28.2°N, 85°W	5173 ± 2124	327.27 ± 134.38	98	333.73 ± 131.69	100
J4	Alaska	59.55°N, 175°W	D7	China	44°N, 125°E	4296 ± 1419	502.55 ± 166.00	53	328.65 ± 118.80	85
V31	Argentina	39.75°S, 55°W	S11	Florida	28.2°N, 85°W	8169 ± 1548	538.81 ± 102.10	94	524.73 ± 96.95	99
V34	Falkland Islands	53.75°S, 55°W	S11	Florida	28.2°N, 85°W	9560 ± 1482	617.42 ± 95.71	96	611.84 ± 92.81	99
T32	Chile	44°S, 75°W	S11	Florida	28.2°N, 85°W	8093 ± 1126	809.3 ± 112.6	62	578.39 ± 93.05	89
AF18	Kenya	4.8°N, 45°E	AD28	South Africa	28.2°S, 25°E	4249 ± 1697	1053.75 ± 420.86	25	373.56 ± 159.75	74

The net cost of storing CO_2 in the ocean for 100 years was estimated by taking the relative efficiency of each site into consideration. This net cost was calculated by multiplying the cost scaling factor (US$6.20/100km /t CO_2 net stored) by the distances between selected injection and high-CO_2 emissions sites, and dividing that cost by the relative efficiency for year 100 in the NO-CLIMATE-CHANGE scenario (Table 3). The net costs of storing buffered CO_2 in the ocean for 100 years was calculated in a similar fashion, except that a cost of US$13.00/t CO_2 was added, and the relative efficiencies at year 100 in the BUFFERED CO_2 scenario was used (Table 3). Based on the dimensions of the GENIE-1 grid cells, each distance and subsequent price has an associated range of uncertainty. The selected site closest to a high emissions region (Z4) has the lowest associated cost of US$82.06 +162.50 -82.06 /t CO_2 net stored without carbonate buffering, and US$75.55 +135.48 -75.55 /t CO_2 net stored with carbonate buffering. Selected site AF18 (off the coast of Kenya) has the highest associated cost of US$1053.75 ± 420.86 /t CO_2 net stored. The high cost of site AF18 is attributed to the low relative efficiency (25%) in the NO-CLIMATE-CHANGE scenario. Selected site V34 (off the Falkland Islands) has the highest cost with carbonate buffering at US$611.84 ± 92.81 /t CO_2 net stored. The high cost of site V34 is credited to the large distance (9560 ±1482 km) from the closest high emissions site. The cost /t CO_2 net stored for the two sites that are within 1,166 km of a major emitting region (Z4 and AE27) range from US$ 82.06 to 89.73/t CO_2 net stored without carbonate buffering, and US$75.55 to 85.31/t CO_2 net stored with carbonate buffering.

4. DISCUSSION

4.1 Controls on Relative Efficiency in Earth System Modeling Experiments

When no social or practical limits are applied, the results demonstrate that relative efficiencies at individual sites in the open ocean largely depend on the state of ocean circulation in different climate change scenarios. The role of ocean circulation is most apparent in the comparisons of NO-CLIMATE-CHANGE and WARMER-CLIMATE scenarios, in which most efficient injection sites in the ocean change from the central North Pacific (in the NO-CLIMATE-CHANGE scenario) to the central North Atlantic (in the WARMER-CLIMATE scenario) by the year 1,000 (Figure 9f, 10f).

The shift in location is related to the change in deep ocean ventilation, which is related to the strength in the Atlantic Meridional Overturning Circulation (AMOC). Ventilation determines the rate that CO_2 is transferred from the surface to the deep ocean, where it sequestered for a longer period of time. Under current conditions, the North Pacific ventilates on the timescale of ~1,000 years, whereas the North Atlantic ventilates more rapidly, on the order of ~300 years [*England,* 1995]. As the ventilation time increases, CO_2 can be stored away from the surface for longer periods of time. Thus, in the NO-CLIMATE-CHANGE scenario where circulation is similar to today, the Pacific deep waters represent the most efficient locations for storing injected CO_2. The shutdown of the AMOC results in the longer ventilation times in the Atlantic basin as well. By year 1,000 in the WARMER-CLIMATE scenario, the North Atlantic displays relative efficiencies similar to those in the North Pacific in the NO-CLIMATE-CHANGE scenario.

This analysis has also examined the interactions between injected liquefied CO_2 and carbonate-bearing sediments in the SEDIMENT-INTERACTION scenario. Carbonate ions are released from dissolving $CaCO_3$ and return to the surface, neutralizing the acidifying effect of CO_2 in the ocean (Appendix A). However, when sediment interactions are included, they only have a small (<5%) effect on the overall relative efficiencies in the SEDIMENT-INTERACTION scenario. One possible reason for this

small impact is the timescale over which the sediment carbonate system is likely to respond to changes in deep water chemistry, i.e. over millennia [*Archer et al.,* 1998]. Other studies using the GENIE-1 model have found that when the interaction between ocean and sediments is included, an additional 12% of CO_2 emissions from the atmosphere are sequestered as bicarbonate ions (HCO_3^-) on a timescale of ~1,700 years [*Ridgwell and Hargreaves,* 2007]. Consequently, the 1,000-year timescale of the experiments in this study was not long enough for larger effects to be observed. Alternatively, when CO_2 is buffered with carbonate at the same time as injection in the BUFFERED-CO_2 scenario, the process of carbonate neutralization begins immediately, and higher relative efficiencies are discernible at all sites for all time periods.

Sites with especially high relative efficiencies in any given scenario would be good candidates for CO_2 injection. However, when more realistic constraints (e.g., the filtering criteria) are applied, many of the open ocean locations with the largest relative efficiencies are removed from consideration. As a result, coastal sites become much more important possibilities for ocean injection.

Coastal sites are the only locations that experience negative relative efficiencies, which occur when CO_2 injection results in more CO_2 being released into the atmosphere (and less in the ocean) than if CO_2 had simply been released straight into the atmosphere (see Figure 8 for example). When CO_2 is released into the atmosphere, it has the possibility of invading the surface ocean at any location in the world. As a result, the CO_2 released into the atmosphere is usually taken in the main regions of the ocean that absorb CO_2, e.g., the North Atlantic surface ocean and the formation regions of Antarctic Intermediate Water in the Southern Hemisphere (*Sabine et al.,* 2004). However, when liquefied CO_2 is injected into a part of the ocean that is not well connected to the deep global ocean circulation (e.g., some coastal areas off Southeast Asia), that CO_2 cannot enter the deep ocean and must first leak into the atmosphere before it is taken up by the surface ocean in another part of the world. When this CO_2 leaks into the atmosphere, it results in a situation where atmospheric CO_2 concentrations are higher in the ocean injection experiment than they are in the CONTROL 2 experiment in which the atmospheric CO_2

has already entered the ocean. In this study, certain sites off the coast of Southeast Asia (Figure 9f, 0-12.8ºS, 120-130ºW) are not well connected to the rest of the deep ocean and hence display large (-10%) negative relative efficiencies by year 1,000 in the NO-CLIMATE-CHANGE scenario. If one were to allow these simulations to continue infinitely, one might expect that any additional carbon dioxide released into the atmosphere would eventually invade the oceans as equilibrium between the ocean and atmosphere system were reached. However, on shorter time scales that are relevant for a 'stop-gap' mitigation of the build-up of atmospheric CO_2, choosing these locations as potential injection sites would worsen the problem of build-up of CO_2 in the atmosphere and ocean. Thus, sites with negative relative efficiencies are important to avoid when considering potential injection sites.

4.2 Experimental Design and Limitations

This study was designed to provide insights about the fate of injected CO_2 in the ocean and atmosphere using different future climate change scenarios, and different injection conditions. This study also represents a sensitivity analysis and as such has certain limitations. For example, in order to isolate the impacts of injected CO_2 on the ocean-atmosphere system, atmospheric CO_2 concentrations were set to pre-industrial levels of 278 ppm and held constant in all scenarios except CONTROL 2. Holding atmospheric CO_2 at a constant, pre-industrial value is obviously an oversimplification of reality as the current average atmospheric concentration of CO_2 is 384.8 ppm, and increasing at an annual rate of 1.6 ppm/y (*Blasin*g, 2009). Increasing atmospheric CO_2 over time in our model simulations would better simulate the invasion of CO_2 into the ocean via natural air-sea gas exchange.

The WARMER-CLIMATE scenario was designed to examine the effects of ocean circulation on relative efficiencies, in the extreme case of a collapse of AMOC. Recent model simulations suggest that the probability of AMOC collapsing in an abrupt (<1 year) fashion is only 10% during the course of the next century [*IPCC*, 2007]. Therefore, a shutdown of AMOC could be considered a rather unlikely occurrence. Nevertheless, the results of this study suggest that even such an extreme circulation change, although

shifting the location of maximum relative efficiency, has a small impact on relative efficiencies overall. In coastal regions where injection sites are most likely to be placed, the differences are minimal.

Another oversimplification in these experiments is the choice of 36.7 Gt CO_2 for injection. This value was chosen because it is traceable throughout the modeled ocean-atmosphere system and would not overwhelm certain geochemical calculations within the model. Although 36.7Gt CO_2 is of the same order of magnitude as the global annual emissions (10 Gt CO_2), it is highly improbable that one could capture this amount of carbon, condense it into liquid form, and consolidate it at one location for injection into the ocean. Currently, the largest CO_2 capture facility can treat a maximum of two tons of CO_2 per hour or 17,500 tons of CO_2/y [*IEA Greenhouse Gas R&D Programme*, 2009]. This rate of production will undoubtedly lengthen the timescale over which CO_2 injection is likely to occur. Even if CO_2 capture technology were improved and expanded in the coming years, it may also be limited to areas with the highest densities of CO_2 emitting power plants. In this case, 530 Mt CO_2/y is the maximum amount of power plant emissions in a given grid cell. Whether this maximum value of CO_2 that could be captured and injected is limited by current carbon capture rates (17,500 tons CO_2/y) or by the regions of the world with high densities of CO_2 producing power plants (530 Mt CO_2/y), ocean CO_2 injection might be better employed as part of a larger mitigation portfolio that includes a host of different carbon sequestration strategies. The limited number of sites suggested by the filtering criteria further supports making ocean storage one part of a portfolio.

The role that ocean storage might play in a mitigation portfolio will also depend on its cost relative to other storage technologies. The costs of ocean storage via pipeline are more than ten times greater than estimated costs provided for any other storage technology (Table 4). The storage technologies considered for comparison represent the major technologies used for geologic sequestration. Enhanced Oil Recovery (EOR) is a process that increases the recovery of oil from a reservoir by injecting CO_2. The respective cost is calculated by the amount of oil produced per production well including the capital cost of the CO_2 recycle plant. It is possible to generate a negative cost (i.e.,

profit) with the by-product credit for the oil extracted. This technology option was included in the comparison to help conceptualize the complete picture of storage projects, and because this technological option is one that is currently developed and utilized in association with oil recovery. For example, the Weyburn Project in Canada's primary objective is EOR, with subsequent storage of CO_2 being an added benefit [*ISEE,* 2008]. I have included this estimate for completeness of comparison, although it is important to note that this calculation does not account for the CO_2 that is generated from the oil that is extracted. Deep oil, gas and saline aquifers can all be used to store CO_2 underground, and deep saline aquifers can store CO_2 underground or below the seabed. Each of these types of reservoirs differs in terms of their pressure, thickness, depth, and permeability. However, the estimated cost of storing CO_2 in these reservoirs is calculated using the same method and is a function of the number of wells and the same reservoir characteristics. Finally, a set of capital, operational, and maintenance costs are used to determine cost, based on the number of wells and a base case overland transport distance (100 km) of CO_2 via pipeline from a power plant to injection site [*Bock et al*., 2003].

Table 4. Costs of CO_2 sequestration technologies [*Bock et al.*, 2003] compared with the average cost of ocean injection estimated in this study

Costs from this study are derived from the average of the two selected injection sites located within 1,166 km of a region of high CO_2 emissions. Costs were estimated from the distances between injection site and emission area using the center point of grid cells.

Storage Option	**US$/t CO_2 net stored**
Enhanced Oil Recovery	-12.21*
Depleted Oil Reservoir	3.82
Depleted Gas Reservoir	4.87
Deep Saline Aquifer	2.93
Ocean Pipeline without Carbonate Neutralization	85.90
Ocean Pipeline with Carbonate Neutralization	80.43

* Number does not account for CO_2 generated when recovered oil is burned.

Ocean storage via pipeline is one of the most expensive storage options available due to large capital costs. Compared to geologic storage, oceanic pipes need to withstand a greater pressure drop per unit of pipeline and be discharged at a pressure equal to the

hydrostatic pressure of the CO_2 inside the pipe. Due to this equal pressure constraint in oceanic injection, a specialized injector unit is needed to discharge CO_2 at the appropriate pressure. This specialized injector unit substantially raises capital costs [*Bock et al.*, 2003]. For comparison, the price of an oceanic injector unit is taken to be $14.5 million [*Ormerod*, 1994] compared to the $966,000 of injection equipment needed for an average oil reservoir injection (calculated) [*Bock et al.*, 2003].

Several factors are likely to influence the costs of ocean CO_2 storage estimated in this study. The first factor concerns the estimation of the distance between sites with high CO_2 emissions and the remaining injection sites. The center of each grid was used as an endpoint, and the grid cells within GENIE-1 are an average of 5,556 km^2 in area. As a result, the actual distance between emission and injection site could fall within a wide range of distances within this grid, and therefore be substantially larger or smaller than the distance estimated between the centers. To address this discrepancy, uncertainty estimates were placed on the distance and subsequent costs of these estimates. These distances range from 920 to 2,219 km. If one considers the maximum estimated distances, then none of the selected sites fall within 1,166 km of the coastline, and therefore no sites would satisfy the current technological constraints of pipeline length. Alternatively, if distances are closer to the minimum values between injection and emission sites, which range from 0 to 1,244 km, then a total of seven sites fall within 1,166 km of the coast and are viable options. It is important to note that at the minimum distance of 0 km, economic costs would still be incurred, and include capital, operational, and maintenance costs.

CO_2 can be buffered using natural carbonates, like limestone. While limestone is globally very abundant, quantities required at the scale of this study (18.35 Gt) may affect the cost of ocean CO_2 sequestration, and mining this amount of limestone could have substantial environmental impacts. This study considered the cost of buffering CO_2 using a constant rate of US$13.00 per ton CO_2 stored, based on the cost of the raw material (limestone), grinding, and shipping [*Golomb et al*., 2007]. In reality, that rate is likely to vary

depending on scarcity of limestone as well as changes in the technology associated with pulverizing and adding limestone to the liquefied CO_2.

Another factor that will likely influence the estimate of cost is identification of regions with highest CO_2 emissions. When identifying the locations of highest densities of CO_2 producing power plants, this study only considered regions where annual emissions exceeded 100 Mt CO_2/y. While the majority of CO_2 capture is likely to take place at these power plants, this identification scheme ignores other point sources of CO_2, such as industry. For example, the cement industry contributes about 5% of global anthropogenic CO_2 emissions [*Worrell et al.,* 2001], and adding point sources of cement production to these emissions estimates increase emissions in some locations of the world. Consideration of regions with emissions greater than 100 Mt CO_2/y accounted for two-thirds of the annual emissions of CO_2 from power plants, which resulted in 30 potential locations. However, if this study were to consider regions with CO_2 emissions greater than 50 Mt CO_2/y, 57 emissions sites become potential regions for the implementation of CO_2 capture technology. These regions include western North America, southeast Australia, Eastern Europe, and south Russia (Figure 14b, d). Only considering power plants greater than 100 Mt CO_2/y is rational based on the perception that the larger emitting power plants are likely to be the first to be retrofitted to capture CO_2. However, if one considers a country such as Canada that emits 550 Mt CO_2/y [*Center for Global Development,* 2007], even capturing 50 Mt CO_2/y of CO_2 makes up nearly 10% of its current annual emissions, and as such could make a significant contribution to a mitigation portfolio.

Several assumptions have also been made when establishing the filtering criteria. For instance, the SOCIO-ENVIRONMENTAL filtering criterion eliminated grid cells containing protected areas [*UNEP-WCMC,* 2009]. These protected areas contain designations such as Biosphere Reserve, Prime Fishing Area and Bird Sanctuary, and therefore include areas with a wide range of management protocols. Pipelines might be permitted in some of these reserves, and could be placed just above the sea floor to minimize habitat disturbance. Excluding the SOCIO-ENVIRONMENTAL criterion allows a closer look at how conservative the results become when we eliminate all grid

cells with protected areas. When examining the results only using the filtering criteria 134, there are 109 potential injection sites (equatorward of 62.7º latitude), compared with the 19 injection sites that remain after applying the 1345 filter. The 109 potential injection sites have a very scattered global distribution. However, large clusters are found adjacent to areas of high emissions in the Mediterranean Sea and off the coasts of Central America, eastern North America, and eastern Asia. Three potential injection sites, in particular, share a common grid cell with high emitting CO_2 sites (Figure 14c). One can consider an even less conservative case by allowing for regions where annual power plant emissions are greater than 50 Mt CO_2 along with the elimination of the socio-environmental filtering criterion. The combined effect is to add 133 sites that would otherwise not have been considered (Figure 14d).

A further complication with this study is the constraint placed on the filtering criteria due to the GENIE-1 grid cell size. For example, when applying the SOCIO-ENVIRONMENTAL criterion, entire grid cells are omitted, and not merely the portion in which the protected area is situated. Real socio-environmental considerations may actually prevent one from selecting an injection site that is within close proximity of an MPA, but it is important to be aware that the filtering procedure used in this study, combined with coarse grid-cell resolution of GENIE-1, results in a conservative, minimum estimate of potential injection sites.

This analysis has only considered ocean injection via pipeline, and therefore the filtering criteria rely heavily upon the technological limitations of ocean pipelines (Figure 12d,f,h,i, and j). The TECHNOLOGICAL filtering criteria are based on the state-of-the-art limitations to pipeline depth and length, but neglect the fact that there has been no previous impetus to build a pipeline any deeper or further from the coast. Thus, the potential to exceed current limits most likely exists and will occur if the need arises. Similarly, this study did not consider ocean injection via tanker or platform. Ocean injection via tanker and platform may in fact be the most cost effective when considering sites greater than 500 km from the coast. The shortest distance between a selected injection site and high emitting CO_2 site in this study is 887 +1757-887 km. At 500 km from a coastline, ocean storage costs US$15.7/t CO_2 net stored from a tanker and

US$13.2/t CO_2 net stored from a platform, compared to US$31.1/t CO_2 net stored by pipeline at 500 km [*IPCC,* 2005]. Therefore, the next step for this study would be to explore the best regions for tanker or platform injection. New considerations might include an examination of potential injection sites that are closest to major ports with high CO_2 emissions and existing platforms.

As mentioned earlier, potential injection sites are on the grid scale based on the resolution of the GENIE-1 model. In an average grid cell area of 5,556 km^2, local effects like eddy activity can affect local mixing of physical properties [*Masuda et al.,* 2009]. These sub-grid-scale processes can affect the distribution of CO_2, which will have an effect on relative efficiency, making it more heterogeneous than is represented by characteristics that are averaged over a large grid cell.

The role of sub-grid-scale processes may also have an effect on the distribution of negative relative efficiencies, which are particular important for determining the effectiveness (and cost) of ocean storage. Results from this study have demonstrated that the sites most likely to be used for ocean storage are found close to the coastlines, but that these are the areas where negative efficiencies occur most frequently. Any errors in the modeled circulation in these coarse-gridded coastal regions could affect estimates of relative efficiencies. If estimates of positive or negative relative efficiencies in these coastal areas are wrong, then injection in these coastal locations could result in the opposite effect than the one desired (i.e., more CO_2 released into the atmosphere on the timescales over which ocean CO_2 injection is needed as short-term mitigation of atmospheric CO_2 buildup). To avoid this outcome, a finer resolution model should be considered in conjunction with research into the known local ocean currents of potential coastal injection sites.

4.3 Future Work

The goal of this paper is to examine how practical ocean storage might be as a mitigation option, in terms of the oceans effectiveness at storing CO_2, but also in terms of its practicality for human society. Although simulations examined 1,000 year timescales, the policy-making process tends to focus on much shorter time periods, on the order of decades. For example, as this paper is being written currently, the United Nations Climate Change Conference of the Parties Meeting (COP15) in Copenhagen is focused on CO_2 reduction targets for 2020, which is less than ten years away. Also, technologically speaking, the canonical "life span" of a coal power plant is on the order of 50 years, with many plants that were built in the 1960s still in operation today. Although the exact time period over which a coal power plant operates might be debated, the point remains that the rate at which our society can transition towards a carbon neutral economy will be limited by technological development, and therefore it seems likely that governments are likely to be placed in the position of seriously considering short-term mitigation options that might help countries to meet their emissions targets and thus slow the effects of anthropogenic climate change. Thus, one way to evaluate the results presented in this study is to examine their potential as a short-term mitigation option.

Even after filtering criteria are applied, the relative efficiencies of selected sites are 66-100% after 50 years, which suggests that ocean injection is a reasonable short-term mitigation option. However, implementation of any large-scale geo-engineering project such as ocean injection of CO_2 will require politicians to create a legal framework through which ocean CO_2 storage will be regulated. Criteria for site selection need to balance the various objectives of the particular ocean storage project. The establishment of such criteria remains one of the main gaps in site selection. Such criteria should consider environmental consequences, costs, safety, injection technology, and international policies and regulations [*IPCC*, 2005]. Other challenges may include monitoring, liability in long-term management, and public acceptance. This study starts to address some of these issues. However, if the costs of ocean injection are ever deemed acceptable, and if this mitigation option is ever pursued, the challenge first remains with

politicians to take these ideas into the political arena and establish targets, objectives, and regulations to implement ocean injection on an international scale.

Environmental impact may be the largest factor determining the acceptability of ocean storage. The overall strategy of ocean injection is rooted in the idea that the impact on the deep ocean would be less than the impacted avoided by limiting emission to the atmosphere. The injection of unbuffered CO_2 is likely to increase the acidity of the ocean [*Doney et al.,* 2009] and many studies have shown the potential impact on organisms, including zooplankton, adult and juvenile fish, and benthic organisms [e.g., *Guinotte and Fabry*, 2008]. Organisms can experience effects ranging from respiratory stress (decreased pH limits oxygen binding and transport of respiratory proteins), and metabolic depression (elevated CO_2 causes some animals to reach a state of motor and or/ mental inactivity), to mortality. Some effects can be reduced through buffering the CO_2 [*Golomb and Angelopoulos*, 2001]. However, more research is needed to quantify these potential effects and to quantify how the impacts of ocean injection of CO_2 are likely to differ from the impacts of ocean acidification of the surface ocean as a result of the business-as-usual CO_2 emissions scenarios.

Interestingly, if the seven coastal locations chosen as potential injection sites in Orr [2004] (Figure 14) were screened using the filtering criteria of this study, not one site would be selected. Six of the seven sites would be eliminated by the SOCIO-ENVIRONMENTAL criteria. This result makes the interesting point that many locations that might be acceptable based on their physical attributes are not acceptable because of their socio-environmental worth, which is perhaps one of the greatest barriers that ocean injection of CO_2 is likely to face in future. The difficulty of ocean storage in respect to social political and regulatory considerations is best highlighted in the view of public precaution toward the ocean. Plans to carry out field tests of ocean storage off Hawaii and later off the Norwegian coast were halted due in large to lobbying from environmental groups [*Keeling*, 2009]. Ocean storage is now banned under the 2006 amendment to the London Protocol for prevention of marine pollution, which classifies CO_2 as a ‘waste’ [*IMO*, 2006]. Protection of the local environment ultimately prevents the collection of

potentially useful data that could outweigh local negative impacts. Such actions prevent collection of data that are pinnacle for policy makers to evaluate prospective large-scale deployment.

Overall, this study has confirmed that ocean storage can only be viewed as a temporary solution to the climate change problem. After 1,000 years nearly all (an average of 100% in the NO-CLIMATE-CHANGE scenario) of the CO_2 has returned to the atmosphere from eligible injection sites. By year 200, 41% of this CO_2 has already escaped to the atmosphere. Thus, the greater challenge to policy makers and society as a whole is to produce a carbon-free economy while mitigation options provide enough time to allow the natural carbon cycle to reduce the atmospheric CO_2 to near pre-industrial levels.

5. CONCLUSIONS

This study examined the natural, practical, socio-environmental, and economic constraints on using ocean CO_2 injection as a potential mitigation strategy for reducing carbon emissions to the atmosphere from power plants. Every site in the ocean was considered as a potential injection site in 1,000-year model experiments using two different climate scenarios: a constant climate (NO-CLIMATE-CHANGE) and an extreme case in which the Atlantic Meridional Overturning Circulation was shut down (WARMER-CLIMATE). Little difference was found between these two simulations for the first 200 years, in both the coastal and open ocean locations. However, after 1,000 years the effect of shutting down the circulation in the North Atlantic Ocean was to shift the location of sites of highest relative efficiency (>70% of original injected CO_2 retained) from the central North Pacific Ocean in the NO-CLIMATE-CHANGE simulation to the central North Atlantic Ocean in the WARMER-CLIMATE scenario. This change resulted from the reduced ventilation of North Atlantic waters allowing the injected CO_2 to remain in the ocean for a longer period of time.

Two sets of experiments in which some form of CO_2 neutralization was implemented: a scenario in which the injected, liquefied CO_2 was allowed to interact with carbonate sediments (SEDIMENT-INTERACTION), and a second scenario in which the liquefied CO2 was injected with a carbonate buffer (BUFFERED-CO_2). The interaction between carbonate sediments and the injected CO_2 had a minimal (<5%) impact on site relative efficiencies, most likely because the timescale of ocean-sediment interactions is quite a bit longer than the time over which our experiments were conducted (1,000 years). In contrast, relative efficiencies were substantially higher at all locations and at all time periods in the BUFFERED-CO_2 scenario when compared with all other scenarios. This result suggests that, in addition to limiting the impacts of ocean acidification, limestone addition makes a substantial difference to the effectiveness and subsequent cost of ocean CO_2 injection.

In order to consider which ocean sites are likely to be most practical for any form of ocean CO_2 injection activities this study also applied several physical, technological, and

environmental filtering criteria. Physical constraints limited sites to depths in the ocean where CO_2 was most likely to remain a liquid and sink to the bottom. Technological criteria considered the state-of-the-art limitations on pipeline lengths, and removed all sites beyond these constraints. Environmental screening criteria eliminated all locations that have been deemed important to society via a classification as a Marine Protected Area. Once these constraints were applied, only 46 sites remained as possibilities - 19 of which were located equatorward of 62.7 degrees latitude. These 19 sites had relative efficiencies ranging from 66 to 100% at 50 years, and 11 to 95% after 200 years in the NO-CLIMATE-CHANGE scenario. By year 1,000 in the same scenario, only 13 of these sites had positive relative efficiencies, ranging from 1 to 9%. The other six sites have negative relative efficiencies, indicated that injection of CO_2 at these locations would actually result in more CO_2 in the atmosphere after 1,000 years. These results therefore indicate injection sites must be selected very cautiously. Furthermore, CO_2 injection has a limited lifespan as a mitigation technology, as almost all of the CO_2 injected would return to the atmosphere after 1,000 years.

Interestingly, relatively little difference in relative efficiency was observed between the NO-CLIMATE-CHANGE, WARMER-CLIMATE and SEDIMENT-INTERACTION scenarios at these selected 19 sites, indicating that the practical constraints to ocean injection provide a greater constraint on this strategy than does the impact of anthropogenic induced climate change. In contrast, the BUFFERED-CO_2 scenario proved to have a marked increase in relative efficiency across these remaining sites. At year 200, these 19 sites had relative efficiencies ranging from 60-98%. The relative efficiencies decreased to 64-80% after by year 1,000. However, this increased relative efficiency comes with an associated cost of limestone addition, which adds an additional US$13.00 per ton CO_2 net stored to the already steep cost of using this technology for seven of the 19 selected sites that have comparable relative efficiencies in the NO-CLIMATE-CHANGE scenario.

While this study demonstrates that relative CO_2 sequestration efficiencies are close to zero after 1,000 years, relative efficiencies are still high (66 to 100 %) at these 19

selected sites over the timescales of 0-50 years, which are relevant timescales for politicians and policy-makers. Thus, it is possible that ocean CO_2 injection might be considered as a stop-gap measure for mitigating high CO_2 emissions while governments work to achieve low-carbon economies in the future. However, in order to use ocean CO_2 injection as a mitigation strategy, politicians must first deal with several legal and regulatory issues that currently stand in the way of large-scale implementation. Furthermore, a more detailed consideration of public safety, environmental health, societal values and economic costs would be required. These political and societal constraints remain as an additional challenge to its implementation.

Finally, the cost of implementing ocean CO_2 injection was estimated by considering only the costs of pumping liquefied CO_2 from high-emitting regions to the potential injection sites, and converting this potential pipeline distance to a cost per ton of CO_2 net stored using a simple scaling factor [*Akai et al.,* 2004]. Although there are large uncertainties associated with this estimation because of the area of the model grid cell (average of 5,556 km^2), first-order estimates of cost per ton CO_2 sequestered is an order of magnitude larger than other CO_2 sequestration technologies considered. While it is possible that these costs may decrease in future due to improvements in technology, based on the current high cost of implementation and the binding constraints of the filtering criteria, this study would not consider ocean CO_2 injection to be competitive in comparison with other technologies.

6. APPENDICES

APPENDIX A. CO_2 in the Ocean

Dissolved minerals in the ocean have made the ocean somewhat alkaline, allowing the mildly acidic CO_2 gas of the atmosphere to be absorbed readily and in large quantities. The exchange of atmospheric CO_2 with ocean surface water is governed by the chemical equilibrium between CO_2 and carbonic acid (H_2CO_3) along with the partial pressure of CO_2 (pCO_2) in the atmosphere and the rate of exchange. H_2CO_3 is further dissociated into bicarbonate ion (HCO_3^-), carbonate ion (CO_3^{2-}) and hydronium ion (H^+).

$$CO_2\ (g) + H_2O <-> H_2CO_3\ (aq) <-> HCO_3- + {}^{+}+ <-> CO_3^{2-} + 2H^+$$

CO_2 in the ocean is measured as total dissolved inorganic carbon (DIC), which is the sum of carbon contained in H_2CO_3, HCO_3^- and CO_3^{2-}. Adding CO_2 will increase DIC, but not total alkalinity (ALK). ALK is defined as the amount of strong acid required to bring sea water to the 'equivalence point' of which the HCO_3^- and H_2CO_3 contributions are equal (Dickson, 1981). The general effect of adding CO_2 to seawater is to form bicarbonate ion, which lowers ocean pH and CO_3^{2-}, but not ALK.

$$CO_2 + H_20 <-> H^+\ HCO_3-$$

ALK is increased when alkaline minerals such as CaCO3 are dissolved in seawater, releasing both DIC and ALK.

$$CaCO_3\ (s) <-> Ca^{2+} + CO_3^{2-}$$

APPENDIX B. Marine Protected Areas

NOTE: These tables are not exhaustive and only aim to illustrate the wide variety of MPA targets/designations/definitions in use.

Number of Marine Protected Areas included in this study separated by their primary management target [adapted from *UNEP-WCMC,* 2009]

Primary Management Target	**Sample Designations/International Conventions**	**Number**
Wildlife (non-fish)	Bird Sanctuary, Dugong Protection Area, Waterfowl Gathering Area	615
Wetlands	Wetlands of International Importance (Ramsar Convention), Wetland Reserve	373
Fishing	Federal Fishing Management Zone, Gear Restricted Area	147
Fish Habitat	Fish Habitat Area, Grouper Spawning Site	116
Flora	Managed Flora Reserve, Virgin Jungle Reserve, State Artificial Reef	96
Cultural	Archeological Reserve, World Heritage Convention,	96
Ecological	Area of Outstanding Ecological Significance, Ecological Conservation Area	76
Multiple	Conservation Area, National Park, UNESCO-MAB Biosphere Reserve	3,190

Definitions of some of the most common designations/international conventions [adapted from *WWF-UK,* 2005]

Designation/Inter-national Convention	**Definition**
National Park	Natural area of land and/or sea, designated to a) protect the ecological integrity of one of more ecosystems for present and future generations, b) exclude exploitation or occupation inimical to the purposes of designation of the area and c) provide a foundation for spiritual, scientific, educational, recreational and visitor opportunities, all of which must be environmentally and culturally compatible.
Fisheries No-Take Zone	A fisheries 'No-Take Zone' (NTZ) is an area of sea that has been temporarily or permanently closed to all (not some gear types) fishing to protect fish stocks and natural habitats. NTZ's can enable the ecosystem within the area to recover (at least partially) from the effects of fishing.
Ramsar Convention	Mission Statement: "The Convention's mission is the conservation and wise use of all wetlands through local, regional and national actions and international cooperation, as a contribution towards achieving sustainable development throughout the world" (*Ramsar COP8*, 2002). Ramsar sites are classified to meet the commitments under the Ramsar Convention. These sites comprise of globally important wetland areas and may extend into the marine environment up to a depth of 6 m.
National Monument	Area containing one, or more, specific natural or natural/cultural feature which is of outstanding or unique value because of its inherent rarity, representative or aesthetic qualities or cultural significance.
Nature Reserve	Areas covered by tidal waters out to territorial limits for the purpose of protecting representative areas of those which contain especially interesting marine fauna and flora or other features.
Habitat/Species Management Area	Area of land and/or sea subject to active intervention for management purposes so as to ensure the maintenance of habitats and/or to meet the requirements of specific species.

APPENDIX C. Gridded Annual CO_2 Emissions

Total annual CO_2 emissions from power plants for year 2007 per GENIE-1 grid, for gridded locations with emissions greater than 100 Mt/CO_2/y [*Center for Global Development,* 2007]

Positive latitude (Lat.) and longitude (Lon.) equate to º North and East respectively. Negative latitude (Lat.) and longitude (Lon) equate to º South and West respectively.

GENIE-1 Grid ID	Lat., Northern Boundary GENIE-1 Grid (º)	Lat., Southern Boundary GENIE-1 Grid (º)	Lon., Western Boundary GENIE-1 Grid (º)	Lon., Eastern Boundary GENIE-1 Grid(º)	Lat., GENIE-1 Grid center (º)	Lon., GENIE-1 Grid center (º)	No. of Power Plants Included in Grid	Total Mt/CO_2/y Emissions in Grid
S8	41.8	37.7	-90	-80	39.75	-85	359	530
C9	37.7	33.7	110	120	35.7	115	130	518
C8	41.8	37.7	110	120	39.75	115	57	311
C10	33.7	30	110	120	31.85	115	72	300
E9	37.7	33.7	130	140	35.7	135	593	256
T8	41.8	37.7	-80	-70	39.75	-75	605	252
S10	33.7	30	-90	-80	31.85	-85	194	243
S9	37.7	33.7	-90	-80	35.7	-85	201	242
AB6	51.1	46.2	0	10	48.65	5	821	211
AA5	56.4	51.1	-10	0	53.75	-5	653	205
AB5	56.4	51.1	0	10	53.75	5	1073	200
D9	37.7	33.7	120	130	35.7	125	101	199
R10	33.7	30	-100	-90	31.85	-95	182	199
AC5	56.4	51.1	10	20	53.75	15	439	188
S7	46.2	41.8	-90	-80	44	-85	427	168
AC6	51.1	46.2	10	20	48.65	15	551	163
R8	41.8	37.7	-100	-90	39.75	-95	242	153
D10	33.7	30	120	130	31.85	125	77	151
C12	26.4	22.9	110	120	24.65	115	83	149

GENIE-1 Grid ID	Lat., Northern Boundary GENIE-1 Grid (º)	Lat., Southern Boundary GENIE-1 Grid (º)	Lon., Western Boundary GENIE-1 Grid (º)	Lon., Eastern Boundary GENIE-1 Grid(º)	Lat., GENIE-1 Grid center (º)	Lon., GENIE-1 Grid center (º)	No. of Power Plants Included in Grid	Total Mt/CO_2/y Emissions in Grid
B11	30	26.4	100	110	28.2	105	45	145
R11	30	26.4	-100	-90	28.2	-95	114	127
C11	30	26.4	110	120	28.2	115	34	125
AJ12	26.4	22.9	80	90	24.65	85	53	124
C13	22.9	19.5	110	120	21.2	115	55	124
AJ13	22.9	19.5	80	90	21.2	85	56	111
D7	46.2	41.8	120	130	44	125	19	103
AD28	-26.4	-30	20	30	-28.2	25	21	103
S11	30	26.4	-90	-80	28.2	-85	95	101
B9	37.7	33.7	100	110	35.7	105	30	101
R9	37.7	33.7	-100	-90	35.7	-95	130	101

7. REFERNCES

Akai, M., N. Nishio, M. Iijima, M. Ozaki, J. Minamiura, and T. Tanaka (2004), Performance and economic evaluation of CO_2 capture and sequestration technologies. Proceedings of the Seventh International Conference on Greenhouse Gas Control Technologies.

Archer, D., H. Kheshgi, and M. Ernst (1998), Dynamics of fossil fuel CO_2 neutralization by marine $CaCO_3$, *Global Biogeochemical Cycles*, 12(2), 259-276.

Bachu, S. (2007), CO_2 in geologic media: role, means, status and barriers to deployment, *Progress in Energy and Combustion Science*, 32(2), 254-273.

Blasing, T. (2009), Recent greenhouse gas concentrations [Available online at: http://cdiac.ornl.gov/pns/current_ghg.html, Accessed December 12th, 2009].

Bock, B., R. Rhudy, H. Herzog, M. Klett, J. Davidson, D. De La Torre Ugarte, and D. Simbeck (2003), Economic Evaluation of CO_2 Storage and Sink Enhancement Options, Final Technical Report, Tennessee Valley Authority Public Power Institute, Muscle Shoals, Alabama, 1-1 – 8-13.

Brewer, P., E. Peltzer, I. Aya, P. Haugan, R. Bellerby, K. Yammane, R. Kojima, P. Walz, and Y. Nakajima (2004) Small scale field study of an ocean CO_2 plume, *Journal of Oceanography*, 60(4), 751-758.

Caldeira, K., and M. Wickett (2005), Ocean model predictions of chemistry changes from carbon dioxide emissions to the atmosphere and ocean, *Journal of Geophysical Research*, 110, C09S04.

Cao, L., M. Eby, A. Ridgwell, K. Caldeira, D. Archer, A. Ishida, F. Joos, K. Matsumoto, U. Mikolajewicz, A. Mouchet, J. Orr, G.-K. Plattner, R. Schlitzer, K. Tokos, I. Totterdell, T. Tschumi, Y. Yamanaka, and A. Yool (2009), The role of ocean transport in the uptake of anthropogenic CO_2, *Biogeosciences*, 6, 375-390.

Center for Global Development (2007), Carbon monitoring for action (CARMA) [Available online at: http://carma.org, Accessed December 12th, 2009].

Clarke, L., M. Wise, J. Edmonds, M. Placed, P. Kyle, K. Calvin, S. Kim, and S. Smith (2008), CO_2 emissions mitigation and technological advance: An updated analysis of advanced technology scenarios, Prepared for the U.S. Department of Energy under Contract DE-AC05-76RL01830, 11pp, Pacific Northwest National Laboratory, Richland, Washington (Scenarios updated January 2009).

Dickson, A. (1981), An exact definition of total alkalinity and a procedure for the estimation of alkalinity and total CO_2 from titration data, *Deep Sea Research Part A*, 28(6), 609-623.

Doney, S., V. Fabry, R. Feely, and J. Kleypas (2009), Ocean acidification: The other CO_2 problem, *Annual Review of Marine Science*, 1, 169-192.

Dooley, J., R. Dahowaski, C. Davidson, M. Wise, N. Gupta, S. Kim, and E. Malone (2006), Carbon dioxide capture and geologic storage, A Technological Report from the Second Phase of the Global Energy Technology Strategy Program, 6pp, Battelle, Joint Global Change Research Institute, College Park, Maryland.

Edmonds, J. (2008). The potential role of CCS in climate stabilization, Plenary Presentation, 9th International Conference on Greenhouse Gas Control Technologies, slide 6 and 14, Washington, DC.

Edwards, N., and R. Marsh (2005), Uncertainties due to transport-parameter sensitivity in an efficient 3-D ocean-climate model, *Climate Dynamics*, 24, 415-433.

England, M. (1995), The age of water and ventilation timescales in a global ocean model, *Journal of Physical Oceanography*, 25, 2756-2777.

GASSCO (2008), Langeled [Available online at: http://www.gassco.no/wps/wcm/connect/gassco-en/Gassco/Home/var-virksomhet/ror-og-plattformer/langeled, Accessed December 1, 2009].

Golomb, D., and A. Angelopoulos (2001), A benign form of CO_2 sequestration in the ocean, Proceedings of the 5th International Conference on Greenhouse Gas Control Technologies. Victoria, Australia: CSIRO Publishing: Collingwood.

Golomb, D., S. Pennell, D. Ryan, E. Barry, and P. Swett (2007), Ocean Sequestration of carbon dioxide: Modeling the deep ocean release of a dense emulsion of liquid CO_2-in-water stabilized by pulverized limestone particles, *Environment Science and Technology*, 41, 4698-4704.

Gough, C., and S. Shackley (2006), Towards a multi-criteria methodology for assessment of geological carbon storage options, *Climatic Change*, 74, 141-174.

Guinotte, J., and V. Fabry (2008), Ocean acidification and its potential effects on marine ecosystems, *New York Academy of Sciences Annals*, 1134, 320-342.

Herzog, H., K. Caldeira, and J. Reilly (2003), An issue of permanence: Assessing the effectiveness of temporary carbon storage, *Climatic Change*, 59, 293-310.

IEA Greenhouse Gas R&D Programme (2009), Castor, "CO_2 from Capture to Storage" [Available online at: http://www.co2captureandstorage.info/project_specific.php?project_id=124, Accessed December 1, 2009].

IMO (2006), New international rules to allow storage of CO2 adopted, IMO Briefing 43/2006, 1, International Maritime Organization, London, UK, November 8th, 2006.

IPCC (2005), IPCC Special Report on Carbon Dioxide Capture and Storage. Prepared by Working Group III of the Intergovernmental Panel on Climate Change, edited by: Metz, B., O. Davidson, H. de Coninck, M. Loos, and L.A. Meyer, Cambridge University Press, Cambridge, UK and New York, USA, 277-317.

IPCC (2007), IPCC Fourth Assessment Report (AR4) "The Physical Science Basis". Prepared by Working Group I if the Intergovernmental Panel on Climate Change, edited by: Solomon, S., D. Qin, M. Manning, Z. Chen, M. Marquis, K.B. Avery, M. Tignor, and H. Miller, Cambridge University Press, New York, 6-243.

ISSE (2008), Carbon Capture and Sequestration Projects [Available online at: http://www.hart-isee.com/index.php?page=carbon-capture-and-sequestration, Accessed December 18, 2009].

Keeling, R. (2009) Triage in the greenhouse, *Nature Geoscience*, 2, 820-822.

Keeney, R., and D. von Winterfeldt, (1994), Managing Nuclear Waste from Power Plants, *Risk Analysis*, 14, 107-130.

Kravitz, B., A. Robock, L. Oman, G. Stenchikov, and A. Marquardt (2009), Sulfuric acid deposition from stratospheric geoengineering with sulfate aerosols, *Journal of Geophysical Research*, in press.

Lynch-Stieglitz, J., J. Adkins, W. Curry, T. Dokken, I. Hall, J. Herguera, J. Hirschi, E. Ivanova, C. Kissel, O. Marchal, T. Marchitto, I. McCave, J. MaManus, S. Mulitza, U. Ninnemann, F. Peeters, E. Yu, and R. Zahn (2007), Atlantic meridional overturning circulation during the last glacial maximum, *Science*, 316, 66-69.

Marchetti, C. (1977), On geoengineering and the CO_2 problem, *Climatic Change*, 1 (1), 59-68.

Masuda, Y., Y. Yamanaka, Y. Sasai, M. Magi, and T. Ohsumi (2009), Site selection in CO_2 ocean sequestration: Dependence of CO_2 injection rate on eddy activity distribution, *International Journal of Greenhouse Gas Control*, *3*, 67-76.

NOAA (2008), Layers of the Ocean, Online School for Weather, [Available online at: http://oceanservice.noaa.gov/education/yos/resource/JetStream/ocean/layers_ocean.htm, Accessed December13th, 2009].

NSIDC (2009), Land and Sea Distribution, [Available online at: http://nsidc.org/arcticmet/factors/land_sea_distribution.html, National Snow and Ice Data Center Education Center, Boulder, Colorado, Accessed: December 18th, 2009].

Ormerod, W. (1994), The disposal of carbon dioxide from fossil fuel fired power stations Technical Report GHG/SR3, 13pp, IEA Greenhouse R&D Programme, Cheltenham, UK.

Orr, J. (2004), Modeling of ocean storage of CO_2 -The GOSAC Study, Report PH4/37, 96, 1-114pp, International Energy Agency, Greenhouse Gas R&D Programme, Cheltenham, UK.

Pruess, K. (2006), On leakage from geologic storage reservoirs of CO_2, Proceedings, 2, CO_2SC Symposium, Berkley, California.

Ramsar COP8 (2002), Assessing and reporting the status and rends of wetlands, and the implementation of Article 3.2 of the Convention concerning change in the ecological character of Ramsar sites, Information Paper, 1pp, 8th Meeting of the Conference of the Contracting Parties to the Convention on Wetlands, Valencia, Spain.

Ridgwell, A., J. Hargreaves, N. Edwards, J. Annan, T. Lenton, R. Marsh, A. Yool, and A. Watson (2007), Marine geochemical data assimilation in an efficient Earth System Model of global biogeochemical cycling, *Biogeosciences*, 4, 87-104.

Ridgwell, A., and J. Hargreaves (2007), Regulation of atmospheric CO_2 by deep-sea sediments in an Earth System Model, *Global Biogeochemical Cycles*, 21, 1-14.

Ridgwell, A., J. S. Singarayer, A. M. Hetherington, and P. Valdes (2009), Tackling regional climate change by leaf albedo bio-geoengineering, *Current Biology* 19, 146-150.

Sabine, C., R. Feely, N. Gruber, R. Key, K. Lee, J. Bullister, R. Wanninkhof, C. Wong, D. Wallace, B. Tilbrook, F. Millero, T-S. Peng, A. Kozyr, T. Ono, and A. Rios (2004), The oceanic sink for anthropogenic CO_2, *Science*, 305, 367-371.

Takeuchi, K., Y. Fujioka, Y. Kawasaki, and Y. Shiryama (1997), Impacts of high concentration of CO_2 on marine organisms: A modification of CO_2 ocean sequestration, *Energy Conservation and Management*, 38, 337-342.

UNEP-WCMC (2008), National and Regional Networks of Marine Protected Areas: A Review of Progress, 1-5pp, United National Environment Programme World Conservation Monitoring Centre, Cambridge, UK.

UNEP-WCMC (2009), World Database on Protected Areas (WDPA) Annual Release 2009, 11-23pp, United National Environment Programme World Conservation Monitoring Centre, Cambridge, UK (Updated: February 2009).

UNESCO-MAB (2008), Dialogue in biosphere reserves: References, practices and experiences, Technical Notes 2, 1pp,United Nations Educational Scientific and Cultural Organization, Paris, France.

Worrell, E., L. Price, C. Hendricks, and L. Ozawa Meida (2001), Carbon dioxide emissions from the global cement industry, *Annual Review of Energy and the Environment*, 26, 303-329.

WWF-UK (2005), MPA designations: A summary of definitions and objectives, Technical Report, 1-8pp, Surrey, UK.

Zhang, Y. (2005), Fate of rising droplets in seawater, *Environmental Science and Technology, 39*, 7719-7724.